2013

Overview of the Large-Scale Biosphere–Atmosphere Experiment in Amazonia Data Model Intercomparison Project (LBA-DMIP)

Luis Gustavo Goncalves de Goncalves
(CPTEC), Instituto Nacional de Pesquisas Espaciais, gustavo.goncalves@cptec.inpe.br

Jordan Borak
University of Maryland, Hydrological Sciences Laboratory, NASA Goddard Space Flight Center, Jordan.Borak@nasa.gov

Marcos Heil Costa
Federal University of Vic¸osa, mhcosta@ufv.br

Scott R. Saleska
University of Arizona, saleska@arizona.edu

Ian Baker
Colorado State University - Fort Collins, baker@atmos.colostate.edu

See next page for additional authors

Authors
Luis Gustavo Goncalves de Goncalves, Jordan Borak, Marcos Heil Costa, Scott R. Saleska, Ian Baker, Natalia Resprepo-Coupe, Michel Nobre Muza, Benjamin Poulter, Hans Verbeeck, Joshua B. Fisher, Altaf Arain, Phillip Arkin, Bruno P. Cestaro, Bradley Christoffersen, David Galbraith, Xiaodan Guan, Bart van den Hurk, Kazuhito Ichii, Hewlley Acioli Imbuzeiro, Atul Jain, Naomi Levine, Chaoqun Lu, Gonzalo Migues-Macho, Debora Roberti, Alok Sahoo, Koichi Sakaguchi, Kevin Shaefer, Mingjie Shi, James Shuttleworth, Hanqin Tian, Zong-Lian Yang, and Xubin Zeng

Agricultural and Forest Meteorology 182–183 (2013) 111–127

Contents lists available at ScienceDirect

Agricultural and Forest Meteorology

journal homepage: www.elsevier.com/locate/agrformet

Overview of the Large-Scale Biosphere–Atmosphere Experiment in Amazonia Data Model Intercomparison Project (LBA-DMIP)

Luis Gustavo Gonçalves de Gonçalves[a,b,*], Jordan S. Borak[c,d], Marcos Heil Costa[e,1], Scott R. Saleska[f], Ian Baker[g], Natalia Restrepo-Coupe[h,f], Michel Nobre Muza[i], Benjamin Poulter[j], Hans Verbeeck[k], Joshua B. Fisher[l,2], M. Altaf Arain[m], Phillip Arkin[n], Bruno P. Cestaro[o], Bradley Christoffersen[f], David Galbraith[p], Xiaodan Guan[q], Bart J.J.M. van den Hurk[r], Kazuhito Ichii[s], Hewlley M. Acioli Imbuzeiro[t], Atul K. Jain[u], Naomi Levine[v], Chaoqun Lu[w], Gonzalo Miguez-Macho[x], Débora R. Roberti[y], Alok Sahoo[z], Koichi Sakaguchi[aa], Kevin Schaefer[bb], Mingjie Shi[cc], W. James Shuttleworth[dd], Hanqin Tian[ee], Zong-Liang Yang[ff], Xubin Zeng[gg]

[a] Centro de Previsão do Tempo e Estudos Climáticos (CPTEC), Cachoeira Paulista, SP, Brazil
[b] Instituto Nacional de Pesquisas Espaciais (INPE), Brazil
[c] Earth System Science Interdisciplinary Center, University of Maryland, College Park, Greenbelt, MD 20740, USA
[d] Hydrological Sciences Laboratory, NASA Goddard Space Flight Center, Code 617, Greenbelt, MD 20771, USA
[e] Department of Agricultural Engineering, Federal University of Viçosa, Viçosa, MG 36570-000, Brazil
[f] Department of Ecology and Evolutionary Biology, University of Arizona, Biosciences West 310, Tucson, AZ 85721, USA
[g] Atmospheric Science Department, 1371 Campus Delivery, Colorado State University, Fort Collins, CO 80523-1371, USA
[h] Plant Functional Biology and Climate Change Cluster, University of Technology, Sydney, Australia
[i] Instituto Federal de Santa Catarina, Florianópolis, SC, Brazil
[j] Laboratoire des Sciences du Climat et l'Environnement (LSCE), Orme des Merisiers, bat. 701 – Point courrier 129, 91191 Gif Sur Yvette, France
[k] Laboratory of Plant Ecology, Faculty of Bioscience Engineering, Ghent University, Coupure Links 653, 9000 Ghent, Belgium
[l] Jet Propulsion Laboratory, California Institute of Technology, 4800 Oak Grove Drive, Pasadena, CA 91109, USA
[m] School of Geography and Earth Sciences, McMaster University, 1280 Main Street West, Hamilton, Ontario, Canada L8S 4K1
[n] Cooperative Institute for Climate and Satellites, Earth System Science Interdisciplinary Center, University of Maryland, College Park, 5825 University Research Court, Suite 4001, College Park, MD 20740-3823, USA
[o] Department of Atmospheric Sciences, University of São Paulo, São Paulo, Brazil
[p] School of Geography, University of Leeds, Leeds LS2 9JT, UK
[q] Key Laboratory of Semi-Arid Climate Change, MOE, College of Atmospheric Sciences, Lanzhou University, China
[r] Royal Netherlands Meteorological Institute, KNMI, PO Box 201, 3730 AE De Bilt, Netherlands
[s] Faculty of Symbiotic Systems Science, Fukushima University, 1 Kanayagawa, Fukushima 960-1296, Japan
[t] Grupo de Pesquisas em Interação Atmosfera-Biosfera, Universidade Federal de Viçosa, MG, Brazil
[u] Department of Atmospheric Sciences, University of Illinois at Urbana-Champaign, 105 South Gregory Street, Urbana, IL 61801, USA
[v] Department of Organismic and Evolutionary Biology, Harvard University, 26 Oxford Street, Cambridge, MA 02138, USA
[w] International Center for Climate and Global Change Research, School of Forestry and Wildlife Sciences, Auburn University Auburn, AL, USA
[x] Nonlinear Physics Group, Universidade de Santiago de Compostela, Santiago de Compostela, Spain
[y] Department of Physics, Federal University of Santa Maria, Santa Maria, Rio Grande do Sul, Brazil
[z] Department of Civil and Environmental Engineering, Princeton University, Princeton, NJ 08544, USA
[aa] Department of Atmospheric Sciences, University of Arizona, Tucson, AZ 85271, USA
[bb] National Snow and Ice Data Center, 449 UCB, University of Colorado, Boulder, CO 80309-0449, USA
[cc] Department of Geological Sciences, Jackson School of Geosciences, The University of Texas at Austin, 1 University Station C1100, Austin, TX 78712, USA
[dd] Department of Hydrology and Water Resources, The University of Arizona, PO Box 210011, Tucson, AZ 85721, USA
[ee] International Center for Climate and Global Change Research, School of Forestry and Wildlife Sciences, Auburn University, 602 Duncan Drive, Auburn, AL 36849, USA
[ff] Center for Integrated Earth System Science, Jackson School of Geosciences, University of Texas at Austin, Austin, TX 78712-0254, USA
[gg] Department of Atmospheric Sciences, The University of Arizona, PO Box 210081, Tucson, AZ 85721, USA

* Corresponding author at: Centro de Previsão do Tempo e Estudos Climáticos (CPTEC), Cachoeira Paulista, SP, Brazil. Tel.: +55 12 3186 8613.
E-mail addresses: gustavo.goncalves@cptec.inpe.br (L.G.G. de Gonçalves), Jordan.Borak@nasa.gov (J.S. Borak), mhcosta@ufv.br (M.H. Costa), saleska@arizona.edu (S.R. Saleska), baker@atmos.colostate.edu (I. Baker), ncoupe@email.arizona.edu (N. Restrepo-Coupe), micmuza@gmail.com (M.N. Muza), Benjamin.Poulter@lsce.ipsl.fr (B. Poulter), Hans.Verbeeck@UGent.be (H. Verbeeck), jbfisher@jpl.nasa.gov (J.B. Fisher), arainm@mcmaster.ca (M.A. Arain), parkin@essic.umd.edu (P. Arkin), brunocesta@gmail.com (B.P. Cestaro), bchristo@arizona.edu (B. Christoffersen), d.r.galbraith@leeds.ac.uk (D. Galbraith), guanxd@lzu.edu.cn (X. Guan), hurkvd@knmi.nl (B.J.J.M. van den Hurk), kazuhito.ichii@gmail.com (K. Ichii), jain1@illinois.edu (A.K. Jain), nlevine@oeb.harvard.edu (N. Levine), CZL0003@auburn.edu (C. Lu), gonzalo.miguez@usc.es (G. Miguez-Macho), debora@ufsm.br (D.R. Roberti), sahoo@princeton.edu (A. Sahoo), ksa@arizona.edu (K. Sakaguchi), kevin.schaefer@nsidc.org (K. Schaefer), mshi.lh@utexas.edu (M. Shi), shuttle@arizona.edu (W.J. Shuttleworth), tianhan@auburn.edu (H. Tian), liang@jsg.utexas.edu (Z.-L. Yang), xubin@atmo.arizona.edu (X. Zeng).
[1] Tel.: +55 31 3899 1899; fax: +55 31 3899 2735.
[2] Tel.: +1 323 540 4569.

0168-1923/$ – see front matter
http://dx.doi.org/10.1016/j.agrformet.2013.04.030

ARTICLE INFO

Article history:
Received 21 August 2012
Received in revised form 28 January 2013
Accepted 10 April 2013

Keywords:
Land surface modeling
Energy, water and carbon budget
Amazonia
Model intercomparison

ABSTRACT

A fundamental question connecting terrestrial ecology and global climate change is the sensitivity of key terrestrial biomes to climatic variability and change. The Amazon region is such a key biome: it contains unparalleled biological diversity, a globally significant store of organic carbon, and it is a potent engine driving global cycles of water and energy. The importance of understanding how land surface dynamics of the Amazon region respond to climatic variability and change is widely appreciated, but despite significant recent advances, large gaps in our understanding remain. Understanding of energy and carbon exchange between terrestrial ecosystems and the atmosphere can be improved through direct observations and experiments, as well as through modeling activities. Land surface/ecosystem models have become important tools for extrapolating local observations and understanding to much larger terrestrial regions. They are also valuable tools to test hypothesis on ecosystem functioning. Funded by NASA under the auspices of the LBA (the Large-Scale Biosphere–Atmosphere Experiment in Amazonia), the LBA Data Model Intercomparison Project (LBA-DMIP) uses a comprehensive data set from an observational network of flux towers across the Amazon, and an ecosystem modeling community engaged in ongoing studies using a suite of different land surface and terrestrial ecosystem models to understand Amazon forest function. Here an overview of this project is presented accompanied by a description of the measurement sites, data, models and protocol.

1. Introduction

The Amazon basin contains the largest area of extant tropical forest on Earth, containing up to 10% of terrestrial biomass (Houghton et al., 2001). Inversion studies suggest tropical Amazonia is a small source of CO_2 to the atmosphere, but uncertainty around this source is so large that in reality the sign of the net flux term is not known (Gurney et al., 2002; Stephens et al., 2007). The net flux is the residual of two large gross fluxes (photosynthetic and respiratory), and influences global CO_2 dynamics. It has been shown that tropical South America exerts considerable influence on global atmospheric CO_2 growth rates (Baker et al., 2006; Bousquet et al., 2000; Rayner et al., 1999; Rödenbeck et al., 2003). Large surface fluxes influence weather both locally (Fu and Li, 2004; Harper et al., 2010; Li and Fu, 2004) and globally (Werth and Avissar, 2002). Clearly, tropical South America plays a significant role in the global circulation and carbon cycle.

Some modeling studies have suggested that within the next 100 years, anthropogenic climate change may force a conversion in tropical South America from evergreen forest to seasonal forest, savanna or grassland (Betts et al., 2004; Cox et al., 2000, 2004; Huntingford et al., 2004, 2008). Under this scenario, carbon released from storage pools to the atmosphere during conversion will impose further changes in radiative forcing in a positive feedback (IPCC, 2007). Other models simulate a continuation of forest function through the end of the 21st century (Friedlingstein et al., 2006).

In a study of climate models participating in the IPCC AR4, Li et al. (2006) found that only 3, of the 11 models studied, predicted reductions in South American precipitation and associated conversion of vegetation type. No significant change in precipitation was predicted in 3 models, and 5 predicted an increase in precipitation over Amazonia. Of the models that do predict vegetation conversion, there is no consensus on the spatial, temporal, and phenological nature of the conversion (Malhi et al., 2008; Salazar et al., 2007).

Since current knowledge is insufficient to resolve the discrepant predictions, it is critical that we better understand the mechanisms of present day forest–climate interactions in Amazonia if we are to understand forest response to future climatic changes. For example, aside from the increase in fires in Amazonia induced by El Niño scale droughts, confident prediction of even the sign of intact forest carbon cycle responses to such droughts is currently not possible.

On annual timescales, ecosystem and land surface models have generally predicted dry-season declines in photosynthesis and/or evapotranspiration in Amazonia (Botta et al., 2002; Dickinson and Henderson-Sellers, 1988; Lee et al., 2005; Nobre et al., 1991; Tian et al., 2000; Werth and Avissar, 2002). But an accumulating suite of direct observations now suggests a different picture: evapotranspiration and photosynthesis in central Amazonia are not uniformly water-limited, at least up to seasonal time scales, but are driven by available energy and sunlight in wetter regions, with water availability playing a larger role where precipitation is less (Costa et al., 2010; da Rocha et al., 2004; Fisher et al., 2009; Saleska et al., 2003; Souza Filho et al., 2005) (Fig. 1).

Understanding of energy and carbon exchange between terrestrial ecosystems and the atmosphere can be improved through direct observations and experiments, as well as through modeling activities. Land surface/ecosystem models have become an important tool for extrapolating local observations and understanding to much larger terrestrial regions. They are also valuable tools to test hypotheses of ecosystem functioning. In this study the question of sensitivity of Amazonia to climate variation is addressed by means of a detailed data and model intercomparison project. This project leverages two key legacies of the LBA (the Large-Scale Biosphere–Atmosphere Experiment in Amazonia): a comprehensive data set from an observational network of flux towers across Amazonia, and a modeling community engaged in ongoing studies using a suite of different land surface and terrestrial ecosystem models to understand Amazon forest function. This comprehensive data set of meteorological data, carbon, energy and water fluxes from sites across Amazonia was used to drive and evaluate the performance of various land surface models whose simulations were brought to this project by a broad community of collaborators. As a result, a comparison of ecosystem model simulations of terrestrial energy, water and CO_2 fluxes with long-term observations of these quantities over the area of Amazonia was performed in order to understand how well these models quantify the land surface process and to assess deficiencies in the models and how they could be improved.

The primary goal of this project is to synthesize and compare the 21 participating land surface ecosystem models to assess current understanding of the energy, water and carbon cycle in Amazonia; a secondary goal is to use our acquired understanding of inter-model differences to generate precise hypotheses that can be tested by future observations and thereby identify mechanisms to improve model performance. To achieve these goals, the LBA-DMIP project was divided into two phases: a site level intercomparison where the models were run only at the tower sites and a regional intercomparison where the models were forced by regional atmospheric data sets. Here we present an overview of the first phase of LBA-DMIP, as an introduction to the papers that follow.

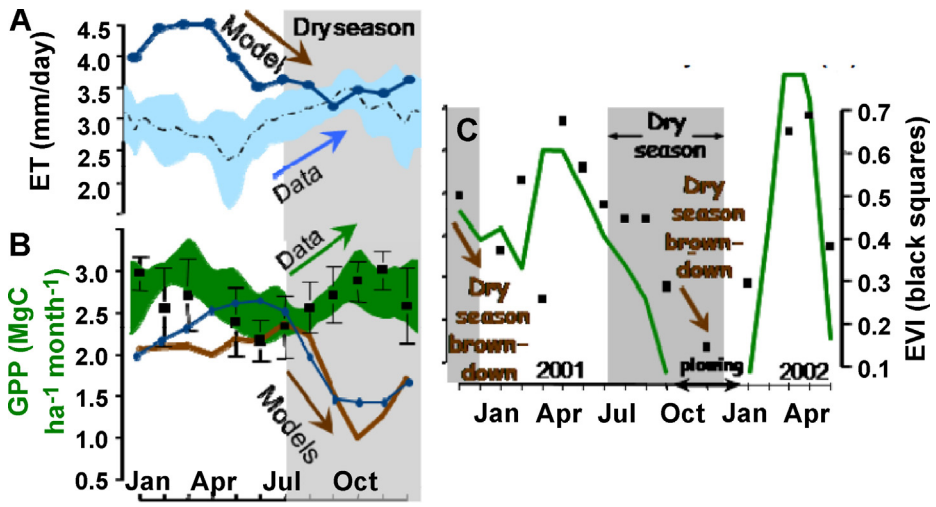

Fig. 1. Local-scale (A) evapotranspiration (ET) and (B) GPP as originally modeled by IBIS (brown line, Botta et al., 2002) and NCAR GCM + Community Land Model (blue line, Lee et al., 2005), and as observed (±SD across years 2002-2004, shaded areas) from eddy tower in Tapajos National Forest (km 67 site). MODIS EVI (average 2000–2004, black squares) is plotted with GPP in (B). Models show dry-season declines, in contrast to observations from both satellite and eddy towers. (C) GPP and EVI in a pasture/agricultural area (km 77 site) that has opposite seasonality from nearby (12 km distant) forest site in (B). (For interpretation of the references to color in this figure legend, the reader is referred to the web version of the article.)

The experiments consisted of uncoupled land surface model simulations forced by standardized atmospheric variables measured at eight sites across the Amazon region as shown in Fig. 2, where each site represents a different biome or a variant of it resulting from disturbance. Section 2 describes the eight sites used in the project. Section 3 describes the gap-filled and quality controlled data, which span eight years of observations. Section 4 presents a detailed description of the 23 different models and their variants that participated in the LBA-DMIP experiments. A detailed common protocol for driving models and reporting simulation results has been produced and its full version is given in Appendix A.

2. Site descriptions

The sites include four evergreen broadleaf forests, a deciduous broadleaf forest, a savanna site, and two pastures. Seven of the eight sites are in Brazilian Amazonia, while a savanna site in the state of São Paulo was also included (Fig. 2).

The evergreen broadleaf forests sites are in the Reserva Biológica do Cuieiras (Cueiras Biological Reserve) near Manaus, Amazonas (the K34 tower); the Floresta Nacional do Tapajós (Tapajós National Forest) near Santarém, Pará (the K67 and K83 towers); the Reserva Jarú (Jarú Reserve) (the RJA tower) located near Ji-Paraná, Rondônia. Manaus K34 is the most western of the central Amazonian sites and is located 60 km north of the city of Manaus (Araújo et al., 2002); it has a dry season from July through September. The Santarém (K67 and K83) forest experimental sites are near the confluence of the Tapajós and Amazon rivers (Hutyra et al., 2007; Miller et al., 2004; Saleska et al., 2003). K67 is in an undisturbed primary forest, but at the K83 site about 15% of the trees with diameter at breast height greater than 35 cm were selectively logged over a 700-ha area during three months starting September 2001 (Figueira et al., 2008; Miller et al., 2007). The Jaru Biological

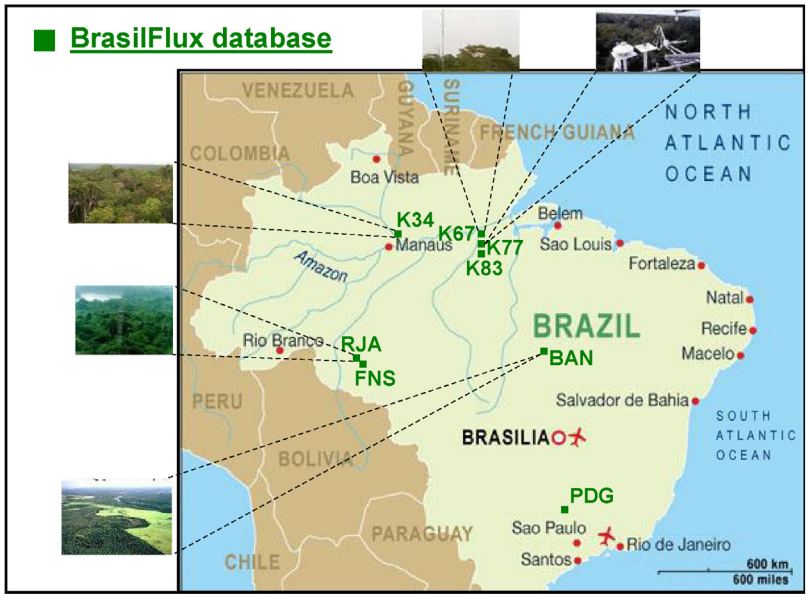

Fig. 2. Flux sites spatial distribution across different ecosystems of Amazonia.

Table 1
Characterization for the eddy covariance tower sites providing driver data for LBA-DMIP (see "Important Note on Data-Use Policy," on the LBA-DMIP Protocol in Appendix A). *Bananal_Island (BAN) also known as JAV*: da Rocha, H. (USP, Brazil) (Borma et al., 2009); *Manaus Km34 (K34)*: Manzi, A., Nobre, A. (INPA, Brazil) (Araújo et al., 2002); *Santarem Km67 (K67)*: Wofsy, S. (Harvard University, USA), Saleska, S. (UofA, USA), Camargo, A. (CENA/USP, Brazil) (Hutyra et al., 2007; Saleska et al., 2003); *Santarem Km83 (K83)*: Goulden M. (UC Irvine, USA), Miller, S. (SUNY, Albany, USA), da Rocha, H. (USP, Brazil). (da Rocha et al., 2004; Goulden et al., 2004; Miller et al., 2004); *Santarem Km77 (K77)*: Fitzjarrald, D. (SUNY, Albany, USA) (Sakai et al., 2004); *Reserva Jaru (RJA)*: Manzi, A. (INPA, Brasil), Cardoso, F. (UFR, Brazil) (Kruijt et al., 2004; von Randow et al., 2004); *Fazenda Nossa Senhora (FNS)*: Waterloo, M. (Vrije Universiteit Amsterdam, The Netherlands), Manzi, A. (INPA, Brazil) (von Randow et al., 2004); *Reserva Pe-de-Gigante (PDG)*: da Rocha, H. (USP, Brazil) (da Rocha et al., 2002).

ID	Short code	Site name	Longitude [°]	Latitude [°]	Elevation [m]	Tower height [m]	Biome type	IGBP class
1	BAN	Bananal Island	−50.1591	−09.8244	120	40	Forest–savanna	4
2	K34	Manaus KM34	−60.2093	−02.6091	130	50	Tropical rainforest	2
3	K67	Santarem KM67	−54.9589	−02.8567	130	63	Moist tropical forest	2
4	K77	Santarem KM77	−54.5365	−03.0119	130	18	Pasture-agriculture	12
5	K83	Santarem KM83	−54.9714	−03.0180	130	64	Selectively logged moist tropical forest	2
6	RJA	Reserva Jaru	−61.9309	−10.0832	191	60	Tropical dry forest	2
7	FNS	Fazenda Nossa Senhora	−62.3572	−10.7618	306	8.5	Pasture	12
8	PDG	Reserva Pe-de-Gigante	−47.6499	−21.6195	690	21	Savanna	9

Reserve site (RJA) is located about 80 km north of Ji-Paraná, Rondônia (Culf et al., 1996). The area contains seasonally dry tropical forest with relatively closed canopy structure and emergent trees. Understory vegetation of only a few meters height consists mainly of palms (Rottenberger et al., 2004). The mean canopy height is 30 m, but the tallest emergent trees reach 44 m (McWilliam et al., 1996).

The deciduous broadleaf forest site is in Ilha do Bananal (BAN). It is a seasonally flooded (forest) ecotone located in the state of Tocantins (Borma et al., 2009) with a 5-month dry season from May through September.

The savanna site is in Reserva Pé-de-Gigante in São Paulo state (PDG savanna tower). Vegetation is a tropical woodland savanna (cerrado) located outside the Amazon basin (da Rocha et al., 2002). It has the longest dry season period of all the sites studied, i.e., 6 months, from April through September. Although this is not an Amazonian site, it has been included in the experiment to allow the assessment of model performance in the cerrado ecosystem.

The pasture sites are the Santarém K77 site and the Rondônia Fazenda Nossa Senhora da Aparecida (FNS) site. K77 is in a previously forested area that had been converted to pasture (grassland). The forest was cleared in 1990, after which the field was planted with the grass *Brachiaria brizantha*. In November 2001 the site was burned and plowed for rice cultivation (Fitzjarrald and Sakai, 2010; Sakai et al., 2004). FNS is a cleared forest located about 30 km northwest of Ji-Paraná (von Randow et al., 2004). This site is in the center of a deforested area with an approximate radius of 50 km – deforestation was caused by a fire in 1977 to clear land for crop cultivation. Since the early 1980s the area has been uniformly covered by *B. brizantha*. The climate there is characterized by annual mean air temperature ranging from 23 to 26 °C, monthly mean precipitation greater than 200 mm from November to April, but less than 20 mm from July to August – and usually less than 5 mm in July (Nobre et al., 1996).

Table 1 presents the main site characteristics while soil properties (textures) for each site are shown in Table 2.

3. Meteorological and flux data

Data are available for three consecutive years for most sites but the period of collection varies from site to site. Santarém K77 has the longest data set of five years whereas at the Pé-de-Gigante (PDG) site there are only two years of data. The data collection period for all sites is between 1999 and 2006. Dry seasons are here defined for all sites as the months with less than 100 mm of long-term mean monthly precipitation (Rosolem et al., 2008), except in the case of the PDG following da Rocha et al. (2009) as the months of April through September. At all sites the dry season is characterized by higher temperatures and an increase in downward shortwave radiation, the exception being PDG where seasonal variations are characteristic of sub-tropical sites with a winter dry season when both temperature and downward shortwave radiation are relatively small (da Rocha et al., 2009).

A number of steps were undertaken to accomplish the proposed objectives of the LBA-DMIP, as follows: (a) meteorological and flux data were acquired from a network of meteorological stations and eddy covariance flux systems in Brazilian Amazonia, to provide a consistently filled continuous data set for driving models; (b) the processed and quality controlled data were used to drive the suite of models; (c) the behavior of the model simulations was compared across models and biomes and (d) the flux observations from (a) were used to test and improve vegetation models of Amazonian carbon and water cycling, for application to projections of climate effects on Amazonian forests. Therefore the core of the LBA-DMIP work used observational evidence – from a variety of ecosystem

Table 2
Site characterization based on soil texture observations: *BAN*: da Rocha, H., personal communication (email February 4, 2009); *K34*: Chambers et al. (2001); *K67*: Williams et al. (2002); *K83:* Keller et al. (2005); *K77*: same as K83; *RJA*: Andreae et al. (2002); *FNS*: same as RJA; *PDG*: da Rocha, H., personal communication (email February 4, 2009).

ID	Short code	% sand	% silt	% clay	Vegetation cover fraction	Canopy height [m]
1	BAN	24	39	37	0.98	16
2	K34	20	12	68	0.98	35
3	K67	2	8	90	0.98	35
4	K77	18	2	80	0–0.8	0–0.6
5	K83	18	2	80	0.98	35
6	RJA	80	10	10	0.98	30
7	FNS	80	10	10	0.85	0.2–0.5
8	PDG	85	12	3	0.80	12

Table 3
Site-specific availability of continuously filled driver data.

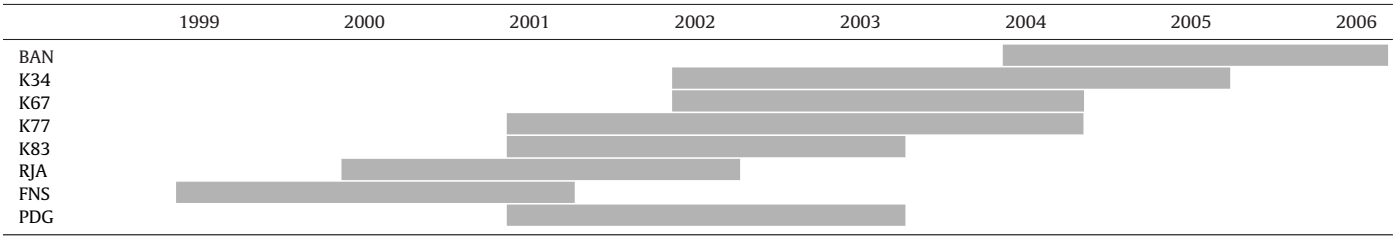

fluxes observed by towers (and where possible, vegetation demography and forest structure) – to drive and test a comprehensive suite of models of Amazonian ecosystem functions.

Continuous driver variables (radiation, temperature, wind, etc.) were created using ALMA-compliant and consistently filled meteorological observations from the eight LBA flux towers described above. ALMA (Assistance for Land-surface Modelling activities) refers to a convention for exchange of data and metadata between land-surface modeling groups that was designed to facilitate consistency and stability, while remaining flexible to future needs (see http://www.lmd.jussieu.fr/~polcher/ALMA for additional details about ALMA). Detailed information about the Principal Investigators (PI) and data references for these tower sites can be found in Appendix A (please refer to "Important Note on Data-Use Policy"). The atmospheric forcing data sets are for periods between 1999 and 2006, the exact time coverage being determined by site-specific data availability as shown in Table 3. The atmospheric variables (forcings) chosen were air temperature, specific humidity, wind speed, downward long wave radiation at the top of the canopy, surface pressure, precipitation, downward shortwave radiation at the top of the canopy and CO_2 concentration (set to 375 ppm). The drivers were provided on a 1-h time-step, linearly interpolated to adjust to each individual model time-step (except for solar radiation, where an interpolation based on the sun zenith angle is more appropriate).

Selected summary statistics for the driver data are presented in Table 4. The forest–savanna site BAN was the warmest, with a mean annual air temperature of 26.4 °C over its period of record, while the savanna site PDG was the coolest at 22.5 °C. Forest sites K34 and RJA were the wettest, with annual mean rainfall totals exceeding 2000 mm, whereas PDG was driest, with an annual rainfall of less than 1300 mm. Associated statistics on gap frequency (Table 4) indicate that data from BAN, K67, FNS and PDG required virtually no gap filling, while both air temperature and precipitation data were missing from K34 and K77 more than 5% of the time. Frequent gaps were found individually in the precipitation and temperature data sets at K83 and RJA, respectively, indicating some degree of independence in gap frequency with respect to data type.

4. Model descriptions

The first phase of the LBA-DMIP simulations included 21 different land surface/ecosystem models representing processes controlling energy, water and carbon cycle dynamics; however, the level of detail with which processes are represented varies across models. Whereas some models are empirically or statistically based with relatively simple relationships between driver variables and fluxes, others are more complex, simulating the coupled carbon, nutrient, and water cycles in terrestrial ecosystems. Models also differ in their representation of soil properties, vegetation type, and environmental forcings, as well as the initialization of carbon pools.

Here we divide the models into three different categories based on their feature sets. Nine models contained non-dynamic representations of vegetation, at time scales varying from hourly to monthly. Of these, five shared the Simple Biosphere Model (SiB – Sellers et al., 1986) as their heritage. Five models included dynamic vegetation and carbon fluxes. An additional six simulated dynamic vegetation, carbon fluxes and nitrogen cycling. See Table 5 for a brief summary of the suite of models used in the LBA-DMIP.

4.1. Models that simulate non-dynamic vegetation

4.1.1. Simple Biosphere Model (SiB) variants

For LBA-DMIP, five model formulations shared the Simple Biosphere Model (SiB) as their heritage. The SiB model was originally introduced by Sellers et al. (1986), and was conceived as a lower boundary for Atmospheric General Circulation Models (AGCMs). The Simplified SiB (SSiB) was designed by Xue et al. (1991) to reduce the physical parameters of SiB, while increasing computational efficiency. It included Jarvis's (1976) empirical approach to estimating stomatal conductance, and did not consider photosynthesis.

The SiB2 model (Sellers et al., 1996) extended the SiB LSM (Sellers et al., 1986), by adding a photosynthesis model and incorporating satellite-based prescription of vegetation phenology, while simplifying its vegetation model by reducing the number of canopy layers from two to one. Its photosynthesis model uses the equations of Farquhar et al. (1980) and Collatz et al. (1991) for C_3 plants,

Table 4
Summary statistics of driver data.

	Air temperature		Precipitation	
	Annual mean (°C)	Annual mean percentage gap-filled	Annual mean (mm)	Annual mean percentage gap-filled
BAN	26.4	0.0	1680.0	0.1
K34	25.6	19.5	2418.5	28.4
K67	25.3	0.0	1597.1	0.3
K77	26.3	6.1	1597.5	7.6
K83	25.9	0.0	1656.2	4.8
RJA	25.1	12.2	2352.9	0.8
FNS	24.7	0.0	1743.9	1.4
PDG	22.5	0.0	1284.6	0.0

Table 5
Summary of models used in the point-based LBA-DMIP simulations.

LBA-DMIP model code	Model name	Affiliation(s) of investigator(s)	Key reference	Energy fluxes (Y/N)?	Water fluxes (Y/N)?	Carbon model (Y/N)?	Nitrogen model (Y/N)?	Dynamic vegetation (Y/N)?
A	SiB2	Federal University of Santa Maria	Sellers et al. (1996)	Y	Y	Y	N	N
B	SiB2 (modified)	University of São Paulo	da Rocha et al. (1996)	Y	Y	Y	N	N
C	SSiB2	Princeton University	Zhan et al. (2003)	Y	Y	Y	N	N
D	SiB3	Colorado State University	Baker et al. (2008)	Y	Y	Y	N	N
E	SiBCASA	National Snow and Ice Data Center	Schaefer et al. (2008)	Y	Y	Y	N	N
F	PT-JPL	Jet Propulsion Laboratory	Fisher et al. (2008)	Y	N	N	N	N
G	H-TESSEL	Royal Netherlands Meteorological Institute	Balsamo et al. (2009)	Y	Y	N	N	N
H	LEAF-Hydro	Universidade de Santiago de Compostela	Miguez-Macho et al. (2007)	Y	Y	N	N	N
I	CN-CLASS	McMaster University	Arain et al. (2006)	Y	Y	Y	Y	N
J	JULES	University of Leeds	Clark et al. (2011)	Y	Y	Y	N	Y
K	Noah-MP	University of Texas	Niu et al. (2011)	Y	Y	Y	N	Y
L	LPJ-WSL	Labatoire des Sciences du Climat et l'Environment	Sitch et al. (2003)	Y	N	Y	N	Y
M	ORCHIDEE	Ghent University	Krinner et al. (2005)	Y	Y	Y	N	Y
N	CLM3.5	University of Arizona	Oleson et al. (2004)	Y	Y	Y	N	N
O	CLM-DGVM	University of Arizona	Levis et al. (2004)	Y	Y	Y	N	Y
P	CLM4CN	University of Texas	Lawrence et al. (2011)	Y	Y	Y	Y	N
Q	IBIS	Universidade Federal de Viçosa	Kucharik et al. (2000)	Y	Y	Y	Y	Y
R	ISAM	University of Illinois	Yang et al. (2009)	Y	Y	Y	Y	Y
S	DLEM	Auburn University	Tian et al. (2010a)	Y	Y	Y	Y	Y
T	Biome-BGC	Fukushima University	Thornton et al. (2002)	Y	Y	Y	Y	Y
U	ED2	Harvard University	Medvigy et al. (2009)	Y	Y	Y	Y	Y

and those of Collatz et al. (1992) for C_4 plants. Canopy conductance follows the methodology of Ball (1988). Fluxes are computed using resistance analogs, so transpiration is determined by the gradient between the saturation vapor pressure of the internal canopy stomata (assuming saturation) and the ambient air, divided by the combined canopy and boundary layer resistances, and scaled by the canopy dry fraction. Only autotrophic respiration of the canopy is considered, and is calculated as a fixed fraction of the maximum leaf photosynthesis rate, which is itself constrained by functions of temperature and soil moisture. The soil is treated as a three-layer substrate, consisting of surface, root, and recharge zones, where direct evaporation occurs, plant roots access moisture, and baseflow plus upward recharge take place, respectively. Phenology and albedo are prescribed from satellite data, and SiB2 contains no biopools or soil pools. Similarly, vegetation dynamics and disturbance are not represented.

A modified version of SiB2 used in LBA-DMIP is specifically calibrated for use within Brazilian biomes (da Rocha et al., 1996). Photosynthesis, conductance and transpiration are calculated in essentially the same way as the original model formulation, with slight modifications related to calibration. The characterization of soil layers is different. The three layers of SiB2 are still present, but the root zone is divided into eight strata, giving a total of 10 soil layers. Phenology dynamics and albedo are still prescribed from satellite (or measured) data, although the equations that parameterize the incident long-wave radiation and the energy balance have been modified in order to calibrate them to the primary Brazilian biomes (da Rocha et al., 1996). As with the original SiB2 model, carbon pools and vegetation dynamics are not considered.

The SSIB2 model (Xue et al., 1991; Zhan et al., 2003) also owes its heritage to SiB, but its formulation reduces the number of physical parameters (like SiB2) and improves computational efficiency. It uses equations similar to those of SiB2 to compute photosynthesis and conductance (Collatz et al., 1991, 1992), with two important distinctions: a) rather than the iterative solution of Sellers et al. (1996a), which is computationally expensive and numerically unstable under certain environmental conditions, it employs a semi-analytical solution and b) it applies Collatz et al.'s (1991,

1992) model separately for sunlit and shaded leaves. Similar to the formulation in SiB2, moisture flux due to canopy transpiration is calculated using a resistance analog where the potential is represented by the gradient between saturation vapor pressure of the canopy and vapor pressure of the canopy air space, along with a prognostically calculated canopy resistance. Autotrophic respiration is explicitly calculated as a function of air temperature, soil moisture, surface-incident shortwave radiation, relative humidity, CO_2 and leaf-area index (LAI), and heterotrophic respiration is not estimated. For its soil model, SSiB2 recognizes 3 layers: surface (0–2 cm), rooting zone (2–150 cm) and drainage/recharge (150–350 cm). As with SiB2, SSiB2 uses satellite data to prescribe its vegetation phenology and albedo. Similarly, the SSiB2 model contains no carbon pools or representation of vegetation dynamics/disturbance.

SiB3 includes several updates to the SiB2 model. Since its introduction, SiB2 has been modified in order to addressed tiling/multiple physiology types (Hanan et al., 2005), prognostic canopy air space (Baker et al., 2003; Vidale and Stöckli, 2005), and tropical forest ecosystems (Baker et al., 2008). As with SiB2, simulated photosynthesis is based on enzyme kinetics (Farquhar et al., 1980), and stomatal conductance couples carbon assimilation to the overall surface energy budget (Collatz et al., 1991, 1992; Randall et al., 1996; Sellers et al., 1996). Stomatal regulation is controlled following the Ball–Berry equations (Ball et al., 1987), with canopy transpiration calculated explicitly on a leaf-level using stomatal conductance and turbulent exchange as described by Sellers et al. (1996). Leaf-to-canopy scaling follows Sellers (1985). Respiration is scaled to balance photosynthesis, following Denning et al. (1996) wherein total respiration is partitioned equally into heterotrophic and autotrophic components, dependent upon soil moisture/soil temperature and fraction of photosynthetically absorbed radiation (fPAR) respectively. The modeled soil depth is 10 m (Baker et al., 2008) and rooting depth follows Jackson et al. (1996). Although SiB3 does not calculate explicit pools, it does parameterize total respiration to balance gross primary productivity (GPP) over the long term. Dynamic vegetation processes, such as succession or vegetation type conversion following disturbance, are not represented. Smaller disturbance is implicitly introduced into the model code through variability in satellite-retrieved spectral indices such as normalized difference vegetation index (NDVI).

The Simple Biosphere/Carnegie-Ames-Stanford Approach (SiBCASA) model (Schaefer et al., 2008, 2009) combines the photosynthesis and biophysical calculations of SiB3 (Baker et al., 2008; Sellers et al., 1996) with the biogeochemistry from CASA (Potter et al., 1993). The photosynthesis and conductance models are similar to SiB2 and consist of a modified Ball–Berry stomatal conductance model (Ball, 1988; Collatz et al., 1991) coupled to a C_3 enzyme kinetic model (Farquhar et al., 1980) and a C_4 photosynthesis model (Collatz et al., 1992). Canopy transpiration is estimated in the same way as SiB3 (Baker et al., 2008). A "Nonstructural Carbohydrates" pool allows SiBCASA to accumulate starch until it is needed, and so SiBCASA has dynamic allocation of carbon between leaf, root, and wood growth. The storage pool and dynamic GPP allocation permit explicit estimation of autotrophic respiration, while heterotrophic respiration is computed using the approach of CASA (Potter et al., 1993). With respect to the soil model, SiBCASA's soil column is 15 m deep, and is divided into 25 layers. The soil thermodynamic model accounts for the effects of organic matter on soil physical properties (Schaefer et al., 2009). SiBCASA's phenology model is semi-prognostic, meaning there is a prognostic leaf biomass and canopy model, but the fPAR is derived from satellite data. SiBCASA has 13 carbon pools, consisting of biomass (leaf, root and woody), surface, soil and storage pools. The model accounts for vegetation dynamics via its semi-prognostic phenology (it is still included in this LBA-DMIP model group due to its clear connection to the original SiB); however, disturbance is not treated and SiBCASA does not account for competition between species or biome types.

4.1.2. Other models that simulate non-dynamic vegetation

Four additional models that simulated only fluxes participated in the LBA-DMIP. They are discussed separately here as they are not direct descendants of the Simple Biosphere Model. This group consists of PT-JPL, H-TESSEL, LEAF-Hydro and CN-CLASS.

The PT-JPL model (Fisher et al., 2008) is a remote sensing-based algorithm designed to retrieve latent heat fluxes (LE). It is based on the Priestley–Taylor (1972) potential evapotranspiration equation, into which Fisher et al. incorporate ecophysiological constraints to reduce potential to actual evapotranspiration. These constraints are functions of atmospheric moisture (vapor pressure deficit and relative humidity) and vegetation indices, specifically NDVI and SAVI (soil-adjusted vegetation index). Because of the foundation of the Priestley–Taylor equation, an advantage of PT-JPL is that it does not require explicit parameterization of stomatal or aerodynamic conductance, which would require a number of assumptions to do so from satellite sensor data. Instead, the complementary hypothesis is invoked so that the constraint functions represent the limits that the resistances would otherwise specify. Canopy transpiration is explicitly calculated starting with the Priestley–Taylor equation, then reducing it with multiplicative constraint functions: relative surface dryness by green canopy fraction; plant temperature constraint; and plant moisture constraint. The model does not consider respiration, and rooting distribution (and subsequent soil moisture) is not required by PT-JPL. Phenology is represented through the temporal sequence and maxima-to-temperature (e.g., optimal growth temperature) pairing using remotely sensed vegetation indices (e.g., NDVI, SAVI). The concepts of carbon pools and vegetation dynamics are not applicable to PT-JPL.

The H-TESSEL (Hydrological-Tiled ECMWF Scheme for Surface Exchange over Land (Balsamo et al., 2009)) model originates from the TESSEL scheme (van den Hurk et al., 2000). The land surface in each tiled atmospheric model grid cell is partitioned amongst bare soil, low and high vegetation, intercepted water, and shaded and exposed snow pack components. For each tile a separate surface energy balance is calculated, but the model has neither representation of dynamic vegetation nor cycling of carbon. H-TESSEL does not consider photosynthetic activity, but it does use a Jarvis (1976) approach for modeling stomatal conductance. The canopy transpiration flux is estimated via a resistance analog. This resistance depends on plant functional type (PFT) and LAI, and is dynamically adjusted depending on available soil moisture, radiation and atmospheric vapor pressure deficit. Respiration is not considered by H-TESSEL. The model's soil is a four-layer column with a root distribution that is defined by PFT-specific exponential equations (Zeng, 2001). The version of H-TESSEL used in the LBA-DMIP project does not consider phenology, biopools or vegetation dynamics.

The LEAF-Hydro model is based on version 2 of LEAF (Land-Ecosystem–Atmosphere-Feedback), the soil–vegetation–atmosphere-transfer scheme in RAMS (Regional Atmosphere Modeling System), a regional climate model developed at Colorado State University. A detailed description of LEAF is given in Walko et al. (2000), with LEAF-Hydro incorporating several hydrological enhancements (Miguez-Macho et al., 2007). These include addition of a prognostic groundwater table, river flow and two-way exchanges of the groundwater store with soil, vegetation and rivers. The model does not simulate photosynthesis; however, it does include a stomatal conductance model, which is described by Lee (1992). Transpiration flux is estimated using a resistance analog, considering the resistance between canopy air space and boundary layer, adjusted by a relative stomatal conductance (Lee et al., 1993). The model does not characterize respiration. For LBA-DMIP,

two soil parameterizations have been used; one set of model runs without a water table and another with a water table. In the absence of an explicitly represented water table, gravitational drainage is the boundary condition at the bottom of the soil column, which is 2.5 m deep. For model runs with a water table, the soil column is 4 m deep. Vegetation phenology is prescribed based on static vegetation type. The albedo is a mix of prescribed vegetation albedo and the bare soil albedo, which depends on soil moisture. Since LEAF does not contain vegetation dynamics, biopools are not present in the model.

The Canadian Land Surface Scheme (CLASS) is a process-based model originally developed by the Meteorological Service of Canada for coupling with the Canadian Global Climate Model (CGCM) and Regional Climate Model (Verseghy, 2000). The Carbon-and-Nitrogen coupled version (CN-CLASS) was developed by incorporating plant and soil carbon, and nitrogen cycle algorithms into CLASS (Arain et al., 2006). CN-CLASS simulates ecological, biophysical and physiological processes (Yuan et al., 2008). Photosynthesis is simulated for sunlit and shaded canopy elements separately (Farquhar et al., 1980), with Vcmax a PFT-dependent function of total RuBisCo-related nitrogen and leaf-area index. Canopy conductance is estimated using a modified form of a Ball–Woodrow–Berry formulation that includes root zone water content effects. CN-CLASS models transpiration via a resistance analog (Verseghy et al., 1993). Autotrophic respiration includes maintenance and growth respiration. Maintenance respiration is a function of live biomass, respiration rate at reference temperature, and temperature sensitivity, employing separate Q10 temperature functions for leaf, stem and root carbon pools. The growth respiration is assumed to be a fixed portion of the net carbon assimilation, after deducting maintenance respiration. Heterotrophic respiration is a function of organic carbon per unit ground area, with a temperature sensitivity defined by a Q10 coefficient, using root zone soil temperature and water content. It is calculated as the sum of CO_2 released from the surface litter layer and the two soil organic matter pools, i.e., "short-lived" and "stable" (Arain et al., 2006). For the LBA-DMIP simulations, the soil column consists of 3 layers that extend to a depth of 4 m. Canopy phenology is prognostic, using thermal formulations (growing degree-days) to determine new leaf growth, with leaf area determination following pipe theory (Shinozaki et al., 1964). Leaf growth is constrained by the supply of assimilate and the transfer of carbon from the assimilate reservoir. Vegetation albedo is calculated as a mean of the values prescribed for each PFT present in the area of interest, weighted by their proportional representation. CN-CLASS contains four vegetation pools (non-structural, leaf, stem and root) and three soil pools (litter, short-lived soil organic matter and stable soil organic matter) (Arain et al., 2006). The version of CN-CLASS used in LBA-DMIP does not include dynamic vegetation.

4.2. Models that simulate dynamic vegetation and carbon fluxes

There were several model participants in the LBA-DMIP that employed both dynamic vegetation and carbon flux components, but did not include nitrogen cycling: JULES, Noah-MP, LPJ-wsl, ORCHIDEE and CLM3.5/CLM-DGVM.

The Joint UK Land Environment Simulator (JULES) model (Clark et al., 2011) is the UK community land surface scheme and is based on the Meteorological Office Surface Exchange Scheme (MOSES) model that has traditionally been used as the land-surface model in the Hadley Centre's climate models. JULES currently is run in combination with the Top-down Representation of Interactive Foliage and Flora Inducing Dynamics (TRIFFID) dynamic vegetation model (Cox, 2001). Photosynthesis is calculated based on the work of Collatz et al. (1991, 1992). Stomatal conductance is coupled to photosynthesis using the approach of Jacobs (1994), which is similar to Leuning's (1995) modification of Ball et al. (1987). A variant of the Penman–Monteith equation is used to derive evapotranspiration, given the aerodynamic and canopy conductances for a given PFT. Maintenance respiration is a function of dark respiration and plant nitrogen content (leaves, roots and stems), while growth respiration is a PFT-dependent fixed fraction of maintenance respiration. Soil respiration is estimated as a function of the soil's carbon concentration, moisture content and a Q10 temperature function (Cox, 2001). The JULES soil column is 3.0 m deep and consists of four layers, with PFT-specific rooting distributions. JULES's canopy phenology is dynamic, with budburst and leaf drop dependent on temperature (Cox, 2001). Surface albedo is calculated as a weighted sum of the spatially prescribed soil albedo and the PFT-prescribed maximum canopy albedo (Cox, 2001). The model's plant carbon pools consist of leaf, root and stem components. Contributions to the litter carbon are derived from the turnover of leaves, roots and stems, as well as a large-scale disturbance term. JULES's use of the TRIFFID DGVM involves a unique Lotka–Volterra population dynamics approach to inter- and intra-species competition (Cox, 2001).

The Noah land surface model with Multi-Parameterization options (Noah-MP) was developed from the original Noah model through community efforts headed by the University of Texas at Austin, the National Centers for Environmental Prediction (NCEP) and the National Center for Atmospheric Research (NCAR). Noah-MP is improved in terms of its mathematical formulations, conceptual realism in biophysical and hydrological processes, and by introducing a framework for multiple options to parameterize selected processes. Relevant feature enhancements include its treatment of the vegetation canopy energy balance, soil moisture–groundwater interaction and related runoff production, and vegetation phenology. For the LBA-DMIP simulations, it employs a Jarvis type stomatal conductance scheme (Chen et al., 1996; Jarvis, 1976) that relates stomatal conductance to photosynthesis of sunlit and shaded leaves (Niu et al., 2011). Calculation of canopy transpiration employs a resistance analog, and it considers separately sunlit vs. shaded vegetation fractions (Niu et al., 2011). Plant maintenance respiration accounts for respiration from leaves, roots, stems and wood, and is a function of a PFT-prescribed maintenance respiration rate, temperature, nitrogen concentration, moisture availability and a respiration reduction factor. Growth respiration for plant tissues derives from prescribed fractions of maintenance respiration. Noah-MP estimates heterotrophic respiration as a function of a soil water and temperature factors for microbial respiration (Yang and Niu, 2003). For the LBA-DMIP runs, the model's soil column is 2 m deep, and consists of four layers. Carbon flux due to leaf phenology is formulated in terms of leaf turnover rate (due to temperature stress, moisture limitation, mechanical loss, or herbivory) (Yang and Niu, 2003), and albedo is prescribed by vegetation type. Noah-MP features four vegetation carbon pools (leaf, stem, root, wood), and two soil carbon pools (fast and slow) (Yang and Niu, 2003). Vegetation dynamics consist of prognostic LAI and greenness fraction as predicted by the phenology model described above (Yang et al., 2011; Yang and Niu, 2003).

LPJ-wsl is a dynamic global vegetation model that simulates coupled biogeography and biogeochemical responses to climate, CO_2, and disturbance (Sitch et al., 2003). Photosynthesis is based on the biophysical approach described by Farquhar et al. (1980) and stomatal conductance constrained by water limitation following Haxeltine and Prentice (1996). Transpiration is estimated as the minimum between potential evaporative demand (Monteith, 1995) and the water supply from two soil layers weighted by root fractions. Maintenance respiration follows a modified Q10 approach (Lloyd and Taylor, 1994) and heterotrophic respiration is both temperature and moisture limited (Foley, 1995). The upper

soil depth is fixed at 0.5 m and the lower depth is 1.0 m (and an additional simulation was conducted with 1.0 and 8.0 m layers), with root fractions PFT specific (e.g., upper soil layer root fraction set to 0.85 for tropical evergreen and 0.60 for tropical raingreen). For the LBA-DMIP work, the associated tropical evergreen phenology assumes no seasonal cycle. Leaf turnover occurs every two years, senescing for the tropical raingreen PFT when soil moisture drops below a critical threshold. Following respiration costs, carbon is allocated to three biomass pools (leaf, sapwood and roots). Vegetation dynamics follow the original approach described by Sitch et al. (2003), with the PFT composition fixed to the vegetation type described for each site, and the fire module disabled for the LBA-MIP simulations.

The ORCHIDEE model (Krinner et al., 2005) consists of a DGVM coupled to the SECHIBA land-surface model (Ducoudré et al., 1993). Its parameterization of photosynthesis follows the formulations of Farquhar et al. (1980) and Collatz et al. (1992), while stomatal conductance is computed via the technique of Ball et al. (1987). As outlined in Ducoudré et al. (1993), transpiration is determined by the gradient of specific humidity between the surface and overlying atmosphere, subject to PFT-specific weightings of surface types. ORCHIDEE's maintenance respiration is calculated using PFT-specific functions of (a) temperature and biomass and (b) nitrogen/carbon ratios (see Ruimy et al., 1996), while its heterotrophic respiration is separately calculated via methods outlined by Parton et al. (1988). Soil layering characteristics are site dependent, with rooting distributions determined by availability of water, light and nitrogen. By definition, vegetation phenology is prognostic and is based on PFT-specific temperature and moisture constraints (Krinner et al., 2005). In addition, ORCHIDEE computes albedo as a weighted average of PFT-prescribed values, combined with a static representation of bare-soil albedo (Krinner et al., 2005). With respect to biopools, the model consists of four separate carbon pools, plus total soil carbon (Verbeeck et al., 2011). Representation of vegetation dynamics and disturbance follows the approach described in the LPJ model (Sitch et al., 2003).

The Community Land Model, version 3.5 (CLM3.5) is a global land-surface model designed to provide surface albedos (direct beam and diffuse for visible and near-infrared wavebands), upward longwave radiation, sensible heat flux, latent heat flux, water vapor flux, and zonal and meridional surface stresses required by atmospheric models (Oleson et al., 2004). As a transition from version 3 to 4 of CLM, CLM3.5 incorporates several modifications to the hydrological cycle, most notably a prognostic unconfined aquifer (Oleson et al., 2008), and improved leaf-to-canopy scaling of photosynthesis. When coupled to a DGVM (as CLM-DGVM), PFT relative abundances become prognostic, the DGVM now bridging PFT-specific gross photosynthesis computed at the grid cell level by CLM with individual-based allometry, following the LPJ concept of an average individual (Levis et al., 2004). C_3 photosynthesis is based on the enzyme-kinetic models of Farquhar et al. (1980), with C_4 photosynthesis derived from the models of Collatz et al. (1992) and Dougherty et al. (1994). An important modification in CLM3.5 was the addition of a nitrogen limitation factor to reduce Vcmax (Oleson et al., 2008). Stomatal conductance is a function of photosynthesis, relative humidity, and CO_2 concentration following the work of Collatz et al. (1991) and Ball et al. (1987), with the exception that gross, instead of net, photosynthesis is used. Sunlit and shaded leaves are treated separately for both photosynthesis and conductance, and are integrated to canopy photosynthesis based on their respective leaf-area indices. Transpiration is a function of the specific humidity gradient between internal leaf surfaces at a given leaf temperature and the atmosphere using a resistance analog in which stomatal leaf boundary layer and atmospheric surface layer resistances act in series, while sunlit and shaded leaf stomatal resistances act in parallel (Oleson et al., 2004). The canopy air space is assumed to have negligible capacity to store water vapor or heat. Atmospheric surface layer resistance is parameterized using Monin–Obukhov similarity theory (Zeng et al., 1998). CLM3.5, without a coupled biogeochemical model such as DGVM or CN, does not simulate respiration. Conversely, CLM-DGVM follows LPJ's approach to modeling autotrophic and heterotrophic respiration (Levis et al., 2004; Sitch et al., 2003). Autotrophic respiration is the sum of maintenance respiration (for leaves, sapwood and roots) and growth respiration, while heterotrophic respiration is modeled as a function of soil moisture and temperature. The CLM soil column is 3.4 m in depth, with 10 layers. Rooting distribution is PFT-dependent and combines both root distribution and maximum rooting depth data using the two-parameter distribution function of Zeng (2001). Albedo is determined by the land-surface model, but phenology can be either satellite-driven for CLM, or prognostic in the case of CLM-DGVM. Carbon pools, absent in the standard version of CLM, are present in CLM-DGVM, and consist of leaf, root, sapwood, heartwood, litter (above and below ground) and soil carbon pools (Levis et al., 2004). Vegetation dynamics in CLM-DGVM include basic treatments of recruitment, three modes of mortality (background rate, heat-induced, and PFT dieback when net annual carbon accumulation is less than zero), competition among PFTs for light and water, and disturbance from fire. Note that separate LBA-DMIP simulations were carried out for CLM3.5 and CLM-DGVM, hence the additional entry in Table 5.

4.3. Models that simulate dynamic vegetation, carbon fluxes and nitrogen cycling

LBA-DMIP included six models that simulate dynamic vegetation, carbon fluxes and nitrogen cycling: CLM4CN, IBIS, ISAM, DLEM, Biome-BGC and ED2.

The Community Land Model, version 4 with carbon and nitrogen biogeochemistry (CLM4CN (Lawrence et al., 2011; Oleson et al., 2010)) builds on CLM3.5 in several ways. The most significant enhancement is the addition of a carbon and nitrogen biogeochemistry module (Randerson et al., 2009; Thornton et al., 2007, 2009) that is based on Biome-BGC (Thornton et al., 2002) and models prognostic carbon and nitrogen in vegetation, litter and soil. Photosynthesis and conductance are essentially unchanged from CLM3.5, except those related to ground evaporation. The parameterization of transpiration is identical to that in CLM3.5. In CLM4CN, autotrophic respiration depends on temperature and tissue nitrogen concentration for live biomass (this excludes dead stem and coarse root pools), and the total heterotrophic demand for mineral nitrogen is expressed as the sum of potential immobilization over all immobilizing steps in a structured pool cascade, as described in Thornton and Rosenbloom (2005). The soil column is extended from 10 to 15 layers; the top 10 are hydrologically active, and identical to those in CLM3.5, while the bottom five layers represent bedrock and are used only for soil thermodynamics (Lawrence et al., 2008). Rooting distribution is modeled as in CLM3.5. Vegetation phenology is prognostic with respect to both carbon and nitrogen, and three distinct phenological types are represented by separated algorithms: an evergreen type, a seasonal-deciduous type, and a stress-deciduous type (Oleson et al., 2010). Representation of surface albedo is unchanged from CLM3.5. CLM4CN includes carbon and nitrogen states for three litter pools, four soil organic matter pools, and a coarse woody debris pool, structured as a converging cascade (as mentioned above in the context of respiration response). Vegetation dynamics updates include the addition of transient land cover/use change (Lawrence and Chase, 2010), and carbon dynamics are controlled by the biogeochemical carbon/nitrogen model. Natural vegetation dynamics are not simulated in CLM4CN (hence the "N" entry in the rightmost column of Table 5), although CLM4CN can be run as part of CLM4's

dynamic global vegetation model known as CNDV (Castillo et al., 2012; Lawrence et al., 2011; Levis et al., 2004; Oleson et al., 2010).

The Integrated Biosphere Simulator (IBIS) model (Foley et al., 1996; Kucharik et al., 2000) was built on the original GENESIS (Global Environmental and Ecological Simulation of Interactive Systems) climate model's Land Surface Transfer scheme, LSX (Levis et al., 1996; Thompson and Pollard, 1995a,b), with the addition of canopy physiological functions, terrestrial carbon cycling and vegetation dynamics. Its stomatal conductance is modeled as a function of the photosynthesis rate, the carbon dioxide concentration and atmospheric humidity (Ball et al., 1987; Leuning, 1995; Lloyd and Farquhar, 1994). Photosynthesis is simulated using the approach of Farquhar et al. (1980), and the equations for photosynthesis and stomatal conductance are closed by the equations of Collatz et al. (1991, 1992). Transpiration flux is modeled as a resistance analog where the canopy conductance is calculated separately for each PFT (Kucharik et al., 2000). Maintenance respiration for leaves is calculated as the product of Vmax and the respiration cost defined by Collatz et al. (1991). For stems, it is calculated as the product of stem carbon content, the Arrenhius temperature function and a maintenance respiration coefficient. Root respiration is similarly defined (Kucharik et al., 2000). Growth respiration is modeled after Amthor (1984), with the carbon lost to growth equal to 30% of net primary productivity. Soil respiration follows the approaches of Lloyd and Taylor (1994) and Linn and Doran (1984) for its temperature and moisture dependency. The IBIS soil consists of six layers in the LBA-DMIP simulations, with a depth ranging from 2 to 8 m across the tower sites. Rooting profiles are defined by "beta" parameters according to Jackson et al. (1996, 1997). IBIS's vegetation phenology module simulates budburst, dormancy and leaf fall using parameterizations that are based on the algorithms of Botta et al. (2000). Model biopools consist of three vegetation pools (leaves, wood and roots) and twelve soil carbon pools. Changes in natural vegetation structure over time are accounted for by using a simple competition method, characterized by the relative abilities of plants to capture light and water from common resource pools in order to fix carbon.

The Integrated Science Assessment Model (ISAM) is a process-based land surface model, with detailed representation of terrestrial biogeochemical and biogeophysical processes, including land use change (LUC) and secondary forest regrowth dynamics (Jain et al., 2009; Jain and Yang, 2005; Yang et al., 2009). Photosynthesis is computed using a coupled "leaf temperature–photosynthesis–stomatal conductance" model (Dai et al., 2004). This utilizes leaf-level photosynthesis models for the C_3 (Collatz et al., 1991; Farquhar et al., 1980) and the C_4 enzyme-kinetic pathways (Collatz et al., 1992), partitioned into sunlit and shaded leaves ("Two big-leaf" formulation). Canopy transpiration is also partitioned into sunlit and shaded components, with each calculated using two tunable parameters: the stomatal conductance slope and the stomatal conductance intercept (Collatz et al., 1991; Dai et al., 2004; Sellers et al., 1996). Autotrophic respiration is the sum of maintenance and growth respirations. Maintenance respiration is calculated separately for leaves, stems, and roots (coarse and fine) using a temperature-dependent Q10 factor (El-Masri et al., 2013). The growth respiration for each pool is assumed to be a fixed percentage (25%) of the difference between GPP and maintenance respiration (Sitch et al., 2003). Heterotrophic respiration is calculated as a sum of carbon release from above and below ground litter and soil carbon pools (Yang et al., 2009). The vertical soil column (approximately 50 m) is represented by 15 layers, which include 10 hydrologically active top layers, and 5 hydrologically inactive bedrock layers (Lawrence et al., 2008). The soil node depths increase exponentially with depth, with a finer resolution in the topsoil to simulate better heat and water transfer in the root zone (Barman et al., 2013). The phenology implemented in the ISAM is based on Arora and Boer (2005) and White et al. (1997), with some modifications to include a water stress factor that triggers senescence for herbaceous biomes (White et al., 1997) and the use of a minimum LAI to indicate the start of the leaf fall period. Surface albedo is prognostic, and is resolved into ground albedo (function of soil color and wetness), exposed vegetation albedo (function of leaf orientation, leaf/stem reflectivity and transmissivity, and ground albedo), and snow albedo. The ISAM recognizes eight vegetation pools and eight litter and soil organic matter pools (El-Masri et al., 2013; Yang et al., 2009). The biogeochemistry component of the ISAM accounts for spatial and temporal patterns of forest and non-forest cover changes, natural fire regimes, and nitrogen deposition, as well as their impacts on plant and soil carbon and nitrogen stocks (Jain et al., 2006, 2009; Jain, 2007; Jain and Yang, 2005; Tao and Jain, 2005; Yang et al., 2009).

The Dynamic Land Ecosystem Model 1.0 (DLEM 1.0) is a highly integrated process-based terrestrial ecosystem model that simulates daily carbon, water and nitrogen cycles driven by changes in atmospheric chemistry (including ozone, nitrogen deposition and CO_2 concentration), climate, land-use and land-cover types and disturbances (Liu et al., 2012; Lu et al., 2011; Ren et al., 2011; Tian et al., 2010a,b, 2011a,b, 2012). DLEM includes five core components: (a) biophysics, (b) plant physiology, (c) soil biogeochemistry, (d) dynamic vegetation and (e) land-use, disturbance and management. Photosynthesis is modeled using a modified Farquhar et al. (1980) approach (Bonan, 1996; Collatz et al., 1991, 1992; Dougherty et al., 1994; Sellers et al., 1996) in which the canopy is divided into sunlit and shaded layers. DLEM 1.0 simulates canopy transpiration using a Penman–Monteith formulation as described in Wigmosta et al. (1994). The model estimates both maintenance and autotrophic growth respiration. Growth respiration is calculated as 25% of all assimilated carbon, while maintenance respiration is related to nitrogen content and adjusted with scalars of temperature and growth season as in the approaches used by Ryan (1991) and Lloyd and Taylor (1994). Soil respiration is controlled by soil temperature, moisture, and available nitrogen for mobilization. DLEM 1.0 has two soil layers, one from the surface down to 50 cm, and the other between 50 cm and 150 cm. Phenology is semi-prognostic, and albedo is prescribed from PFT. The DLEM 1.0 model distinguishes six vegetation carbon pools (storage organ, leaf, heartwood, sapwood, fine root, and coarse root) for trees and shrubs, five vegetation carbon pools (storage organ, leaf, stem, fine root, and coarse root) for herbaceous vegetation, and three soil carbon pools, plus an additional seven pools for litter. As mentioned above, DLEM 1.0 simulates vegetation dynamics (e.g., mortality, senescence) and disturbances (e.g., fire, land-use change, blow-downs).

Biome-BGC (Biogeochemical Cycles) prognostically simulates fluxes of energy, water, carbon and nitrogen for vegetation, litter and soil pools (Thornton et al., 2002). It uses the Farquhar et al. (1980) approach for photosynthesis and a Jarvis-type model (Jarvis, 1976) for stomatal conductance. Transpiration is estimated using the Penman–Monteith equation, and depends on leaf-scale aerodynamic conductance as well as stomatal conductance (Thornton et al., 2002). Autotrophic respiration is partitioned into maintenance respiration – calculated as a function of nitrogen content in vegetation pools, air or soil temperature – and growth respiration, which is a simple proportion of total new carbon allocated to growth. Heterotrophic respiration is calculated as a function of soil temperature, moisture and carbon content. The Biome-BGC model has a single soil water pool, and does not include a vertical soil water layer, root hydraulic redistribution, or vertical distribution of root density. Canopy phenology is prognostic, such that seasonal growth consists of growth stored from the previous season displayed in the current season, as well as current growth (Thornton et al., 2002). Albedo is prescribed following the PFT-based estimates of Dorman and Sellers (1989). Biome-BGC includes a total of seven

vegetation pools, four litter pools and four soil pools. The vegetation type is prognostic, with the model simulating structural changes over time via interacting functions of disturbance history, meteorology, and prescribed ecophysiological vegetation characteristics. The LBA-DMIP simulations used the default Biome-BGC ecophysiological parameter set (White et al., 2000), except in the case of the evergreen broadleaf forest PFT (Ichii et al., 2007).

Version 2 of the Ecosystem Demography Biosphere Model (ED2) is an integrated terrestrial biosphere model incorporating hydrology, land-surface biophysics, vegetation dynamics and soil carbon and nitrogen biogeochemistry (Medvigy et al., 2009; Moorcroft et al., 2001). C_3 photosynthesis follows the approach of Farquhar and Sharkey (1982), while C_4 carbon assimilation is modeled after the work of Collatz et al. (1992). Stomatal conductance is coupled to photosynthesis using the model of Leuning (1995). Transpiration is a function of stomatal resistance and water supply and demand. It is calculated as the sum of open-stomate and closed-stomate transpiration rates, weighted by the relative proportions of each in the canopy. The proportion of open stomata is computed as the ratio of water supply to the sum total of water supply and demand, and the proportion of closed stomata is the remainder. Maintenance respiration for autotrophs is partitioned into leaf, root and storage components. Leaf respiration and leaf turnover are treated separately in ED2; the former is a cost of photosynthesis, and the latter is a maintenance cost which is related to leaf drop. Thus, leaf maintenance is calculated as the (PFT-based) leaf turnover rate multiplied by leaf biomass, adjusted by a temperature dependency. Similarly for roots, maintenance respiration is estimated as the root turnover rate (also PFT-prescribed) multiplied by root biomass, again adjusted for temperature dependency. In the case of the tropical biomes studied in LBA-DMIP, storage maintenance is set to a constant value of zero. Growth respiration is calculated as the product of daily carbon gain and a PFT-dependent growth respiration proportion. Soil respiration is moisture and temperature limited. The ED2 soil properties are based on Cosby et al. (1984). Soil depth is site specific, and rooting depth is a function of tree height (Schenk and Jackson, 2002). Water is extracted from the soil relative to the demand of the individual plant and the root biomass. Vegetation phenology is fully prognostic in the model, not constrained by satellite data. For tropical environments such as in the LBA-DMIP study, drought-deciduous trees can drop their leaves when soil moisture falls below a certain threshold value. Albedo is calculated from the two-stream radiative transfer model, as well as soil type and moisture. ED2 has three active carbon pools that are allocated on a daily basis: leaf, fine roots and sapwood. There is also a storage pool which holds excess carbon. In addition, there is a structural (stem) pool which is grown every month from the storage pool provided that the vegetation is not under drought stress. Four soil pools are discerned, consisting of fast soil carbon, structural soil carbon, structural soil lignin and slow soil carbon. With respect to vegetation dynamics, ED2 is a size- and age-structured model and includes both anthropogenic (although not included in the LBA-MIP runs) and natural disturbances such as fire and wind throw. Individuals compete directly against one another for light and water resources, and both density independent and density dependent mortality are imposed.

5. Conclusions

This overview paper presents a detailed description of the data, models and methods that define the foundation for LBA-DMIP. The project was motivated by the following overarching questions: (a) When do different LSMs produce better simulations when driven by identical meteorological inputs? (b) How do models with different complexities reproduce diurnal, seasonal and annual cycles of surface fluxes? What are the magnitudes of uncertainties? (c) How are land surface process controlled by water, energy and carbon fluxes? (d) What is the partitioning, variance, spatial distribution, and interannual variability of water and energy fluxes in response to atmospheric drivers? (e) What are the links between soil processes and drier climate over Amazon? (f) What can we learn from LSMs about the interactions between water, energy and carbon in the forest–savanna–pasture ecosystem?

This work paved the way for a number of studies aimed at improving the understanding of the sensitivity of Amazonia to climate variation, addressed by means of a detailed data intercomparison. It was conducted by the modeling community using a suite of land surface and terrestrial ecosystem models. From analysis of field data and comparison of modeled terrestrial energy, water and CO_2 fluxes with long-term observations of these quantities, a number of general conclusions can be drawn from a selected list of companion papers and other publications.

1. Restrepo et al. (this issue) conducted a cross-site analysis of flux-tower measurements in order to gain insight into the spatial and seasonal patterns of photosynthetic activity across the Amazon basin as well as the effects of land-use conversion on it. They found that ecosystem-level photosynthesis, as represented by gross ecosystem production (GEP), is not seasonally water-limited in equatorial Amazonian forests. Conversely, seasonal patterns of GEP consistent with increasing water stresses emerge as one transitions southeastward to drier forests (due in part to shallower soils and a weaker relationship between evapotranspiration and net radiation), then on to converted pastures, and finally savanna. Their results suggest that the seasonality of GEP in undisturbed tropical forest ecosystems is driven by complex covariance of adaptive mechanisms (e.g., timing of leaf flush/fall; rooting depth) and sunlight availability, rather than simple variations in water or sunlight availability. Their study also emphasizes the importance of maintaining long-term eddy flux observations in the Amazonia, especially in conjunction with associated biometric measurements, including leaf litterfall and woody increment measurements.
2. Incorporating both flux-tower data and outputs from the full suite of LBA-DMIP participant models, von Randow et al. (this issue) concentrated on carbon and water fluxes at the tower sites. They looked at modeled annual totals of NEE and ET, as well as their interannual variability, which frequently were found to be different from what was observed at the towers. On the other hand, means of the simulated outputs tended to respond similarly to what was observed in the tower, with notable exceptions: (a) observed interannual variability of NEE was mainly influenced by annual precipitation at the forest sites, but simulated interannual variability was driven by both annual precipitation and radiation; (b) interannual variability of ET is strongly controlled by annual variations of radiation, a relationship that is well-captured by the mean of the models. These findings suggest that future climate scenarios of decreases in precipitation could weaken terrestrial CO_2 uptake in Amazonia, so although surface models are able to reproduce, to some extent, these general responses, more development is still necessary in their representations of interannual variability.
3. Focusing on the behavior of a single land surface model, El-Masri et al. (2013) used flux-tower observations to improve ISAM's estimates of carbon fluxes and stocks at eight of the tower sites. They calibrated the model with data from K34 for testing at four additional forest sites, and from FNS for one additional pasture site (PDG was used as both a calibration and test site as it was the only savanna flux tower). Modeled estimates of total biomass ranged from 0.9 to 20.8 kg C/m^2/year for pasture (K77) and forest (K34) sites, respectively. Nearly all forest sites, except for K67,

had lower ratios of NPP:GPP (0.4) than the savanna and pasture sites, which are 0.5. They hypothesized that the ratio at K67 is elevated due to higher NPP. Estimates of soil carbon were lowest at K77 (pasture) and highest at the K34 forest site. All forests sites were found to be net sinks for CO_2, while PDG and FNS (savanna and pasture) were neutral, and K77 was a net source of carbon. ISAM's accurate representation of soil carbon dynamics was illustrated by agreement to the flux-tower measurements within 4.5%, and in fact, all simulated carbon fluxes from ISAM fell within the uncertainty ranges of the tower data, although the authors point out that seasonal variations in leaf-litter production still need work.

4. Baker et al. (this issue) also concentrated on simulations from a single land surface model, SiB3. Their intents were (a) to demonstrate the ability to capture mean annual cycles of biophysical behavior across vegetation and moisture gradients and (b) use SiB3's ability to partition processes in order to formulate more detailed descriptions of mechanisms in model simulations. They used SiB3 outputs of latent heat, sensible heat, and carbon fluxes. These were compared against observations from five tower sites: K34, K67, K83, RJA and PDG. Their results suggested that in the northwest (K34), ecosystems are light limited, with consistently low Bowen ratios and carbon fluxes that are determined by high-frequency variability in light and moisture availability (i.e., no seasonality). Moving southeast, the dry season length was more clearly defined, with a dry-season carbon sink evident in both modeled and observed data. This was due to increased photosynthetic production (greater availability of light) and decreased respiratory efflux (drier soils). In still-drier regions, water and carbon fluxes were in-phase, with carbon uptake during the rainy season and loss during the dry season. At the driest site (PDG), a large annual cycle in latent and sensible heat fluxes was also evident. Overall, there were no consistent biases present in net radiation or latent heat flux; however, there was a positive bias in sensible heat flux across all tower sites. Given the minimum of localized model tuning performed, these were certainly encouraging results.
5. Although it is common to use a single site example of a PFT to generalize for multiple sites, multi-site calibration is achievable in the case of a small number of relatively homogeneous sites. Fischer et al. (this issue) conducted such a calibration for a single PFT (pasture) at FNS and K77. They designed 20 objective functions that consisted of five adjustment measures (i.e., cost functions) to be combined with four parameter-weighting scenarios (just FNS, just K77, their unweighted mean, and their mean weighted proportionally to data series length). All were evaluated to investigate the consistency and sensitivity of NEE as simulated by the SITE land surface model (Santos and Costa, 2004). They noted that the choice of objective function should be based on the intended use, and found that for short time scales, unweighted means combined with mean-absolute error as an adjustment measure performed best. For longer time scales, an unweighted mean combined with the maximum bias error adjustment measure was preferable.
6. The network of meteorological data was used to drive a suite of land surface ecosystem models to investigate what controls ET, and in particular how well models capture the observed diurnal and seasonal cycles of ET across sites. In assessing mechanisms responsible for differences in model performance, it was found that soil moisture storage capacity was an important factor in ability of models to match observed seasonal cycles. Soil moisture storage capacity is not routinely measured at all flux tower sites, but such measurements could improve the ability to discriminate empirically among different model mechanisms used to match observed seasonal patterns (Christoffersen and the LBA-DMIP & BrasilFlux Team, 2009).

In summary, this collection of papers, along with others appearing elsewhere, answers some of the overarching questions, though not all. The LBA-DMIP was an international effort organized around a NASA funded project through its Terrestrial Ecology Program, but moreover it brought together a number of groups and individuals from the international ecobiogeochemistry modeling community dedicated to improving the understanding of how the Amazon works given its diverse ecosystem. It is likely that there will be new science originating from this project for many years, and this set of articles represents one in a series of building blocks.

Acknowledgements

Financial support comes from NASA Terrestrial Ecology Program Grant NNX09AL52G. Research contributed by J.B. Fisher was carried out at the Jet Propulsion Laboratory, California Institute of Technology, under a contract with NASA. We thank the various individuals and modeling groups from Brazil, United States, Canada, Netherlands, England, Japan, Spain among other countries that, with limited or no funding sources, kindly devoted their time and efforts to the success of this project. We also thank the LBA scientists who obtained observations in the field including the Principal Investigators for the tower sites referenced as follows.

K34: Manzi, A., Nobre, A. (Instituto Nacional de Pesquisas da Amazônia (INPA), Brazil) (Araújo et al., 2002)
K67: Wofsy, S. (Harvard University, USA), Saleska, S. (University of Arizona, USA), Camargo, A. CENA/University of São Paulo, Brazil). (Hutyra et al., 2007; Saleska et al., 2003)
K83: Goulden M. (University of California, Irvine, USA), Miller, S. (State University of New York, Albany, USA), da Rocha, H. (University of São Paulo, Brazil) (da Rocha et al., 2004; Goulden et al., 2004; Miller et al., 2004)
K77: Fitzjarrald, D. (State University of New York, Albany, USA) (Sakai et al., 2004)
RJA: Manzi, A. (INPA, Brazil), Cardoso, F. (UFR, Brazil) (Kruijt et al., 2004; von Randow et al., 2004)
FNS: Waterloo, M. (Vrije Universiteit Amsterdam, The Netherlands), Manzi, A. (INPA, Brazil) (von Randow et al., 2004)
BAN: da Rocha, H. (University of São Paulo, Brazil) (Borma et al., 2009)
PDG: da Rocha, H. (University of São Paulo, Brazil) (da Rocha et al., 2002) which have shed much light on the Amazon water cycle and provided data for validating the models.

Appendix A. Data and modeling protocols

1. Atmospheric forcing data sets

   The forcing data are ALMA-compliant, multi-year consistently filled meteorological observations from selected LBA flux towers (BrasilFlux network), including boundary conditions (site location, biome type, soil type and initial data). The data are for periods between 1999 and 2006 in UTC 00:00 time, the exact time coverage being determined by site-specific data availability (see Table 3). Forcing data sets include:
   a. air temperature
   b. specific humidity
   c. wind speed
   d. downward long wave radiation at the surface
   e. surface pressure
   f. precipitation
   g. shortwave downward radiation at the surface
   h. CO_2 is set to 375 ppm

These atmospheric drivers are provided at 1-h time-step as ALMA-compliant ASCII and NetCDF format files. Models use linear interpolation (except for solar radiation, where zenith angle would be more appropriate) if they are run at shorter than a 1 h time step. These data are available from the LBA-MIP website.

2. Phenological information

Models with dynamic vegetation (DGVMs) are run in the mode in which they generate their own phenology (e.g., leaf-area index, LAI), and the value of LAI is reported in the outputs. To facilitate inclusion of those models which cannot prognostically simulate dynamic vegetation structure and phenology, a standard set of monthly LAI values derived by a phenology model (Stöckli et al., 2008) or MODIS-derived phenological information are provided. It should be recognized that known remote sensing technical and physical uncertainties mean these data may be unreliable. However, to minimize these effects, aggregations of the best quality filtered satellite phenological information are derived for each tower site. To facilitate comparison between models and to explore the effect of differences between dynamic vegetation model-derived and MODIS-derived vegetation phenologies, DGVMs are run in two modes if possible: i.e. in prognostic mode (in which leaf phenology is simulated) and in forced mode (in which model phenology is forced by values derived from the MODIS or phenology-model (Stöckli et al., 2008)). As not all sites allow for constant LAI values (e.g., PDG or FNS), participants are encouraged to use LAI values in the following priority: modeled LAI, MODIS-derived monthly LAI and then MODIS-derived constant LAI.

3. Vegetation structure

A few of the eddy flux sites also have data on vegetation structure, for example: aboveground live biomass and biomass increment, litterfall rates, stocks of coarse wood debris, and soil respiration.

4. Initialization and spin-up

Model physics and biophysics are initialized as follows:

a. Soil moisture in all layers set to 0.95 of saturation (porosity).
b. Soil temperature in all layers set to the mean of the yearly air temperature.
c. Because reliable carbon and nitrogen pool observations are not available, soil carbon, living biomass, etc. are spun up according to the best practices for each model, and the spin up procedure used is documented.
d. Initial CO_2 values are assumed as steady-state.

Spin-up for model physics and biogeochemistry use one of the following procedures:

a. Replicate the driving data set to achieve a 10–15 year simulation run.
b. Replicating the driver data set until the mean monthly soil moisture does not deviate by more than 0.1% from the previous year.

5. Model output

Output is provided at 1-h time-step, in UTC time in NetCDF for the variables listed below. The values of state variables are given at the end of each time-step, fluxes are averaged values over a time-step, and storage change variables are accumulated over each time-step.

a. Model states and outputs
   i. Carbon fluxes: GPP, NPP, and Re.
   ii. Energy balance and hydrology: sensible and latent heat flux, net radiation for short and long wave, and runoff.
   iii. Surface soil temperature and soil temperature by layer.
   iv. Soil moisture at the surface and soil moisture by layer.
   v. Soil carbon (total, and by pools where possible, including separate litter pool).
   vi. Input parameters, re-output at the time resolution to simplify analysis.
   vii. Parameters table used for soil description at each site and run, as well as other model assumptions (e.g. rooting depth).
b. Vegetation dynamics (if applicable)
   i. Vegetation carbon (total, leaves, roots, woods, etc. if possible).
   ii. Tree mortality, recruitment, and growth (in carbon flux and as annual rates) broken down by components if possible (total, leaves, roots, and wood).

If a variable is not deliverable, it is replaced by the value of −999.99 that represents either undefined or missing value.

Model diagnostic variables comply with the following radiation energy and water conservation equations. Participants are required to check against these before submitting their results. This ensures that diagnostics, units and timings of the submitted results are appropriate for the analysis. For radiation:

$$SWnet + LWnet - Qh - Qle - Qg = \frac{DelCanh}{dt}$$

where *SWnet*, *LWnet*, *Qh*, *Qle*, and *Qg* represent net short-wave radiation, net long-wave radiation, sensible heat flux, latent heat flux, and ground heat flux, respectively, in W/m^2. The right-hand term, *DelCanh*/*dt*, is the canopy heat storage flux (also in W/m^2).

Water balance (residual at all times is less than 1×10^{-6} $kg/m^2/s$):

$$Rainf + Snowf - Evap - Qs - Qsb + Qrec = \frac{DelIntercept + DelSrfStor + DelSoilMoist}{dt}$$

where *Rainf*, *Snowf*, *Evap*, *Qs*, *Qsb* and *Qrec* are the rates (in kg/m^2) of rainfall, snowfall, total evapotranspiration, surface runoff, subsurface runoff, and recharge. The term on the right-hand side of the equation, (*DelIntercept* + *DelSrfStor* + *DelSoilMoist*)/*dt*, is the rate of change in storage for interception, surface water, and soil moisture, respectively (in $kg/m^2/s$). For the LBA towers neither snow nor ice is separately diagnosed since these states are not likely to occur. Where this is a problem for closing the energy and water balance above, snow states and fluxes are added to respective water state and flux variables. If a model needs additional diagnostic radiation, heat and water storage terms (e.g. canopy air space water and heat storage) on the right-hand side of the above equations, they are added to the diagnostic output and noted appropriately.

6. Important Note on Data-Use Policy

In accordance with LBA data sharing policy these data are freely available to all LBA researchers (http://www.lbaeco.org/lbaeco/data/data_poldoc.htm; see policy #2). Note, in particular, that policy #7 states that:

> *Where data are used for modeling or integrating studies, the scientist collecting the data will be credited appropriately, either by co-authorship or by citation. The data collectors should be informed of publication plans well in advance of submission of a paper, given an opportunity to read the manuscript, and be offered co-authorship. In cases where data from other investigators are a minor contribution to a paper, the data should be referenced by a citation. Users of the data will always have to state the source of the data.*

Please note that, notwithstanding the availability of this common driver data set, the LBA data sharing policy still requires any author or presenter of this data to contact and appropriately credit PIs from individual projects that generated the data used. The necessary contact information is given in Table 1.

References

Amthor, J.S., 1984. The role of maintenance respiration in plant growth. Plant Cell Environ. 7 (8), 561–569.

Andreae, M.O., Artaxo, P., Brandão, C., Carswell, F.E., Ciccioli, P., da Costa, A.L., Culf, A.D., Esteves, J.L., Gash, J.H.C., Grace, J., Kabat, P., Lelieveld, J., Malhi, Y., Manzi, A.O., Meixner, F.X., Nobre, A.D., Nobre, C., Ruivo, M.d.L.P., Silva-Dias, M.A., Stefani, P., Valentini, R., von Jouanne, J., Waterloo, M.J., 2002. Biogeochemical cycling of carbon, water, energy, trace gases, and aerosols in Amazonia: the LBA-EUSTACH experiments. J. Geophys. Res. 107 (D20), 8066.

Arain, M.A., Yuan, F., Black, T.A., 2006. Soil–plant nitrogen cycling modulated carbon exchanges in a western temperate conifer forest in Canada. Agric. For. Meteorol. 140 (1–4), 171–192.

Araújo, A.C., Nobre, A.D., Kruijt, B., Elbers, J.A., Dallarosa, R., Stefani, P., von Randow, C., Manzi, A.O., Culf, A.D., Gash, J.H.C., Valentini, R., Kabat, P., 2002. Comparative measurements of carbon dioxide fluxes from two nearby towers in a central Amazonian rainforest: the Manaus LBA site. J. Geophys. Res. 107 (D20), 8090.

Arora, V.K., Boer, G.J., 2005. A parameterization of leaf phenology for the terrestrial ecosystem component of climate models. Global Change Biol. 11 (1), 39–59.

Baker, D.F., Law, R.M., Gurney, K.R., Rayner, P., Peylin, P., Denning, A.S., Bousquet, P., Bruhwiler, L., Chen, Y.H., Ciais, P., Fung, I.Y., Heimann, M., John, J., Maki, T., Maksyutov, S., Masarie, K., Prather, M., Pak, B., Taguchi, S., Zhu, Z., 2006. TransCom 3 inversion intercomparison: impact of transport model errors on the interannual variability of regional CO_2 fluxes, 1988–2003. Global Biogeochem. Cycles 20 (1), GB1002.

Baker, I., Denning, A.S., Hanan, N., Prihodko, L., Uliasz, M., Vidale, P.-L., Davis, K., Bakwin, P., 2003. Simulated and observed fluxes of sensible and latent heat and CO_2 at the WLEF-TV tower using SiB2.5. Global Change Biol. 9 (9), 1262–1277.

Baker, I.T., Prihodko, L., Denning, A.S., Goulden, M., Miller, S., da Rocha, H.R., 2008. Seasonal drought stress in the Amazon: reconciling models and observations. J. Geophys. Res. 113 (G1), G00B01.

Ball, J.T., 1988. The ci/cs Ratio: A Basis for Predicting Stomatal Control of Photosynthesis. Stanford University, Palo Alto, CA, USA.

Ball, J.T., Woodrow, I.E., Berry, J.A., 1987. A model predicting stomatal conductance and its contribution to the control of photosynthesis under different environmental conditions. In: Biggins, J. (Ed.), Progress in Photosynthesis Research. Martinus Nijhoff Publishers, Dordrecht, Netherlands, pp. 221–224.

Balsamo, G., Beljaars, A., Scipal, K., Viterbo, P., van den Hurk, B., Hirschi, M., Betts, A.K., 2009. A revised hydrology for the ECMWF model: verification from field site to terrestrial water storage and impact in the integrated forecast system. J. Hydrometeorol. 10 (3), 623–643.

Barman, R., El-Masri, B., Song, Y., Meiyappan, P., Jain, A.K., 2013. Climate driven uncertainties in terrestrial energy, water and carbon fluxes: an analysis using a land surface model and eddy covariance measurements across multiple ecosystems. Global Change Biol. (submitted for publication).

Betts, R.A., Cox, P.M., Collins, M., Harris, P.P., Huntingford, C., Jones, C.D., 2004. The role of ecosystem–atmosphere interactions in simulated Amazonian precipitation decrease and forest dieback under global climate warming. Theor. Appl. Climatol. 78 (1–3), 157–175.

Bonan, G., 1996. The NCAR Land Surface Model (LSM Version 1.0) Coupled to the NCAR Community Climate Model. National Center for Atmospheric Research, Boulder, CO, USA.

Borma, L.S., da Rocha, H.R., Cabral, O.M., von Randow, C., Collicchio, E., Kurzatkowski, D., Brugger, P.J., Freitas, H., Tannus, R., Oliveira, L., Rennó, C.D., Artaxo, P., 2009. Atmosphere and hydrological controls of the evapotranspiration over a floodplain forest in the Bananal Island region. Amazonia. J. Geophys. Res. 114 (G1), G01003.

Botta, A., Ramankutty, N., Foley, J.A., 2002. Long-term variations of climate and carbon fluxes over the Amazon basin. Geophys. Res. Lett. 29 (9), 1319.

Botta, A., Viovy, N., Ciais, P., Friedlingstein, P., Monfray, P., 2000. A global prognostic scheme of leaf onset using satellite data. Global Change Biol. 6 (7), 709–725.

Bousquet, P., Peylin, P., Ciais, P., Le Quéré, C., Friedlingstein, P., Tans, P.P., 2000. Regional changes in carbon dioxide fluxes of land and oceans since 1980. Science 290 (5495), 1342–1346.

Castillo, C.K.G., Levis, S., Thornton, P., 2012. Evaluation of the new CNDV option of the Community Land Model: effects of dynamic vegetation and interactive nitrogen on CLM4 means and variability. J. Clim. 25 (11), 3702–3714.

Chambers, J.Q., Santos J. d. Ribeiro, R.J., Higuchi, N., 2001. Tree damage, allometric relationships, and above-ground net primary production in central Amazon forest. Forest Ecol. Manage. 152 (1–3), 73–84.

Chen, F., Mitchell, K., Schaake, J., Xue, Y., Pan, H.-L., Koren, V., Duan, Q.Y., Ek, M., Betts, A., Mitchell, K., Schaake, J., Xue, Y., Pan, H.-L., Koren, V., Duan, Q.Y., Ek, M., Betts, A., 1996. Modeling of land surface evaporation by four schemes and comparison with FIFE observations. J. Geophys. Res. 101 (D3), 7251–7268.

Christoffersen, B., the LBA-DMIP & BrasilFlux Team, 2009. Radiation and available water controls on modeled evapotranspirationacross eight Amazonian flux tower sites: results from the LBA-MIP. Geophys. Res. Abstr. 11, 6386.

Clark, D.B., Mercado, L.M., Sitch, S., Jones, C.D., Gedney, N., Best, M.J., Pryor, M., Rooney, G.G., Essery, R.L.H., Blyth, E., Boucher, O., Harding, R.J., Huntingford, C., Cox, P.M., 2011. The Joint UK Land Environment Simulator (JULES), model description – Part 2: Carbon fluxes and vegetation dynamics. Geosci. Model Dev. 4 (3), 701–722.

Collatz, G.J., Ball, J.T., Grivet, C., Berry, J.A., 1991. Physiological and environmental regulation of stomatal conductance, photosynthesis and transpiration: a model that includes a laminar boundary layer. Agric. For. Meteorol. 54 (2–4), 107–136.

Collatz, G.J., Ribas-Carbo, M., Berry, J.A., 1992. Coupled photosynthesis–stomatal conductance model for leaves of C_4 plants. Aust. J. Plant Physiol. 19 (5), 519–538.

Cosby, B.J., Hornberger, G.M., Clapp, R.B., Ginn, T.R., 1984. A statistical exploration of the relationships of soil moisture characteristics to the physical properties of soils. Water Resour. Res. 20 (6), 682–690.

Costa, M.H., Biajoli, M.C., Sanches, L., Malhado, A.C.M., Hutyra, L.R., da Rocha, H.R., Aguiar, R.G., de Araújo, A.C., 2010. Atmospheric versus vegetation controls of Amazonian tropical rain forest evapotranspiration: are the wet and seasonally dry rain forests any different? J. Geophys. Res. 115 (G4), G04021.

Cox, P.M., 2001. Description of the TRIFFID Dynamic Global Vegetation Model. Hadley Centre Meteorological Office, Exeter, UK.

Cox, P.M., Betts, R.A., Collins, M., Harris, P.P., Huntingford, C., Jones, C.D., 2004. Amazonian forest dieback under climate–carbon cycle projections for the 21st century. Theor. Appl. Climatol. 78 (1), 137–156.

Cox, P.M., Betts, R.A., Jones, C.D., Spall, S.A., Totterdell, I.J., 2000. Acceleration of global warming due to carbon-cycle feedbacks in a coupled climate model. Nature 408 (6809), 184–187.

Culf, A.D., Esteves, J.L., Marques Filho, A.d.O., da Rocha, H.R., 1996. Radiation, temperature and humidity over forest and pasture in Amazonia. In: Gash, J.H.C., Nobre, C.A., Roberts, J.M., Victoria, R.L. (Eds.), Amazonian Deforestation and Climate. J.M. Wiley and Sons, New York, NY, USA, pp. 175–192.

da Rocha, H.R., da Rocha, H.R., Freitas, H.C., Rosolem, R., Juárez, R.I.N., Tannus, R.N., Ligo, M.A., Cabral, O.M.R., Silva Dias, M.A., 2002. Measurements of CO_2 exchange over a woodland savanna (Cerrado Sensu stricto) in southeast Brasil. Biota Neotrop. 2 (1).

da Rocha, H.R., Goulden, M.L., Miller, S.D., Menton, M.C., Pinto, L.D.V.O., de Freitas, H.C., e Silva Figueira, A.M., 2004. Seasonality of water and heat fluxes over a tropical forest in eastern Amazonia. Ecol. Appl. 14 (sp4), 22–32.

da Rocha, H.R., Manzi, A.O., Cabral, O.M., Miller, S.D., Goulden, M.L., Saleska, S.R., R.-Coupe, N., Wofsy, S.C., Borma, L.S., Artaxo, P., Vourlitis, G., Nogueira, J.S., Cardoso, F.L., Nobre, A.D., Kruijt, B., Freitas, H.C., von Randow, C., Aguiar, R.G., Maia, J.F., 2009. Patterns of water and heat flux across a biome gradient from tropical forest to savanna in Brazil. J. Geophys. Res. 114 (G1), G00B12.

da Rocha, H.R., Sellers, P.J., Collatz, G.J., Wright, I.R., Grace, J., 1996. Calibration and use of the SiB2 model to estimate water vapour and carbon exchange at the ABRACOS forest sites. In: Gash, J.H.C., Nobre, C.A., Roberts, J.M., Victoria, R.L. (Eds.), Amazonian Deforestation and Climate. John Wiley and Sons, pp. 459–472.

Dai, Y., Dickinson, R.E., Wang, Y.-P., 2004. A two-big-leaf model for canopy temperature, photosynthesis, and stomatal conductance. J. Clim. 17 (12), 2281–2299.

Denning, A.S., Collatz, G.J., Zhang, C., Randall, D.A., Berry, J.A., Sellers, P.J., Colell, G.D., Dazlich, D.A., 1996. Simulations of terrestrial carbon metabolism and atmospheric CO_2 in a general circulation model. Tellus B 48 (4), 521–542.

Dickinson, R.E., Henderson-Sellers, A., 1988. Modelling tropical deforestation: a study of GCM land-surface parametrizations. Quart. J. Roy. Meteorol. Soc. 114 (480), 439–462.

Dorman, J.L., Sellers, P.J., 1989. A global climatology of albedo, roughness length and stomatal resistance for atmospheric general circulation models as represented by the Simple Biosphere Model (SiB). J. Appl. Meteorol. 28 (9), 833–855.

Dougherty, R.L., Bradford, J.A., Coyne, P.I., Sims, P.L., 1994. Applying an empirical model of stomatal conductance to three C-4 grasses. Agric. For. Meteorol. 67 (3/4), 269–290.

Ducoudré, N.I., Laval, K., Perrier, A., 1993. SECHIBA, a new set of parameterizations of the hydrologic exchanges at the land-atmosphere interface within the LMD atmospheric general circulation model. J. Clim. 6 (2), 248–273.

El-Masri, B., Barman, R., Meiyappan, P., Song, Y., Liang1, M., Jain, A.K., 2013. Carbon dynamics in the Amazonian Basin: fusion of eddy covariance and ecophysiological data with a land surface model. Agric. For. Meteorol. 182–183, 156–167.

Farquhar, G.D., Caemmerer, S., Berry, J.A., 1980. A biochemical model of photosynthetic CO_2 assimilation in leaves of C3 species. Planta 149 (1), 78–90.

Farquhar, G.D., Sharkey, T.D., 1982. Stomatal conductance and photosynthesis. Annu. Rev. Plant Phys. 33 (1), 317–345.

Figueira, A.M.e.S., Miller, S.D., de Sousa, C.A.D., Menton, M.C., Maia, A.R., da Rocha, H.R., Goulden, M.L., 2008. Effects of selective logging on tropical forest tree growth. J. Geophys. Res. 113 (G1), G00B05.

Fisher, J.B., Malhi, Y., Bonal, D., Da Rocha, H.R., De Araújo, A.C., Gamo, M., Goulden, M.L., Hirano, T., Huete, A.R., Kondo, H., Kumagai, T.O., Loescher, H.W., Miller, S., Nobre, A.D., Nouvellon, Y., Oberbauer, S.F., Panuthai, S., Roupsard, O., Saleska, S., Tanaka, K., Tanaka, N., Tu, K.P., von Randow, C., 2009. The land–atmosphere water flux in the tropics. Global Change Biol. 15 (11), 2694–2714.

Fisher, J.B., Tu, K.P., Baldocchi, D.D., 2008. Global estimates of the land–atmosphere water flux based on monthly AVHRR and ISLSCP-II data, validated at 16 FLUXNET sites. Remote Sens. Environ. 112 (3), 901–919.

Fitzjarrald, D.R., Sakai, R.K., 2010. LBA-ECO CD-03 Flux-Meteorological Data, km 77 Pasture Site, Para, Brazil: 2000–2005. Data Set.

Foley, J.A., 1995. An equilibrium model of the terrestrial carbon budget. Tellus B 47 (3), 310–319.

Foley, J.A., Prentice, I.C., Ramankutty, N., Levis, S., Pollard, D., Sitch, S., Haxeltine, A., 1996. An integrated biosphere model of land surface processes, terrestrial carbon balance, and vegetation dynamics. Global Biogeochem. Cycles 10 (4), 603–628.

Friedlingstein, P., Cox, P., Betts, R., Bopp, L., von Bloh, W., Brovkin, V., Cadule, P., Doney, S., Eby, M., Fung, I., Bala, G., John, J., Jones, C., Joos, F., Kato, T., Kawamiya, M., Knorr, W., Lindsay, K., Matthews, H.D., Raddatz, T., Rayner, P., Reick, C., Roeckner, E., Schnitzler, K.G., Schnur, R., Strassmann, K., Weaver, A.J., Yoshikawa, C.,

Zeng, N., 2006. Climate–carbon cycle feedback analysis: results from the C4MIP model intercomparison. J. Clim. 19 (14), 3337–3353.
Fu, R., Li, W., 2004. The influence of the land surface on the transition from dry to wet season in Amazonia. Theor. Appl. Climatol. 78 (1), 97–110.
Goulden, M.L., Miller, S.D., da Rocha, H.R., Menton, M.C., de Freitas, H.C., e Silva Figueira, A.M., de Sousa, C.A.D., 2004. Diel and seasonal patterns of tropical forest CO_2 exchange. Ecol. Appl. 14 (sp4), 42–54.
Gurney, K.R., Law, R.M., Denning, A.S., Rayner, P.J., Baker, D., Bousquet, P., Bruhwiler, L., Chen, Y.-H., Ciais, P., Fan, S., Fung, I.Y., Gloor, M., Heimann, M., Higuchi, K., John, J., Maki, T., Maksyutov, S., Masarie, K., Peylin, P., Prather, M., Pak, B.C., Randerson, J., Sarmiento, J., Taguchi, S., Takahashi, T., Yuen, C.-W., 2002. Towards robust regional estimates of CO_2 sources and sinks using atmospheric transport models. Nature 415 (6872), 626–630.
Hanan, N.P., Berry, J.A., Verma, S.B., Walter-Shea, E.A., Suyker, A.E., Burba, G.G., Denning, A.S., 2005. Testing a model of CO_2, water and energy exchange in Great Plains tallgrass prairie and wheat ecosystems. Agric. For. Meteorol. 131 (3/4), 162–179.
Harper, A.B., Denning, A.S., Baker, I.T., Branson, M.D., Prihodko, L., Randall, D.A., 2010. Role of deep soil moisture in modulating climate in the Amazon rainforest. Geophys. Res. Lett. 37 (5), L05802.
Haxeltine, A., Prentice, I.C., 1996. BIOME3: an equilibrium terrestrial biosphere model based on ecophysiological constraints, resource availability, and competition among plant functional types. Global Biogeochem. Cycles 10 (4), 693–709.
Houghton, R.A., Lawrence, K.T., Hackler, J.L., Brown, S., 2001. The spatial distribution of forest biomass in the Brazilian Amazon: a comparison of estimates. Global Change Biol. 7 (7), 731–746.
Huntingford, C., Fisher, R.A., Mercado, L., Booth, B.B.B., Sitch, S., Harris, P.P., Cox, P.M., Jones, C.D., Betts, R.A., Malhi, Y., Harris, G.R., Collins, M., Moorcroft, P., 2008. Towards quantifying uncertainty in predictions of Amazon 'dieback'. Philos. Trans. R. Soc. Lond. Ser. B 363 (1498), 1857–1864.
Huntingford, C., Harris, P.P., Gedney, N., Cox, P.M., Betts, R.A., Marengo, J.A., Gash, J.H.C., 2004. Using a GCM analogue model to investigate the potential for Amazonian forest dieback. Theor. Appl. Climatol. 78 (1), 177–185.
Hutyra, L.R., Munger, J.W., Saleska, S.R., Gottlieb, E., Daube, B.C., Dunn, A.L., Amaral, D.F., de Camargo, P.B., Wofsy, S.C., 2007. Seasonal controls on the exchange of carbon and water in an Amazonian rain forest. J. Geophys. Res. 112 (G3), G03008.
Ichii, K., Hashimoto, H., White, M.A., Potter, C., Hutyra, L.R., Huete, A.R., Myneni, R.B., Nemani, R.R., 2007. Constraining rooting depths in tropical rainforests using satellite data and ecosystem modeling for accurate simulation of gross primary production seasonality. Global Change Biol. 13 (1), 67–77.
IPCC, 2007. Climate Change 2007: The Physical Science Basis. Contribution of Working Group I to the Fourth Assessment Report of the Intergovernmental Panel on Climate Change, Cambridge, United Kingdom/New York, NY, USA.
Jackson, R.B., Canadell, J., Ehleringer, J.R., Mooney, H.A., Sala, O.E., Schulze, E.D., 1996. A global analysis of root distributions for terrestrial biomes. Oecologia 108 (3), 389–411.
Jackson, R.B., Mooney, H.A., Schulze, E.D., 1997. A global budget for fine root biomass, surface area, and nutrient contents. Proc. Natl. Acad. Sci. U.S.A. 94 (14), 7362–7366.
Jacobs, C.M.J., 1994. Direct Impact of Atmospheric CO_2 Enrichment on Regional Transpiration. Wageningen Agricultural University, Netherlands, pp. 179.
Jain, A., Yang, X., Kheshgi, H., McGuire, A.D., Post, W., Kicklighter, D., 2009. Nitrogen attenuation of terrestrial carbon cycle response to global environmental factors. Global Biogeochem. Cycles 23 (4), GB4028.
Jain, A.K., 2007. Global estimation of CO emissions using three sets of satellite data for burned area. Atmos Environ. 41 (33), 6931–6940.
Jain, A.K., Tao, Z., Yang, X., Gillespie, C., 2006. Estimates of global biomass burning emissions for reactive greenhouse gases (CO NMHCs and NOx) and CO_2. J. Geophys. Res. 111 (D6), D06304.
Jain, A.K., Yang, X., 2005. Modeling the effects of two different land cover change data sets on the carbon stocks of plants and soils in concert with CO_2 and climate change. Global Biogeochem. Cycles 19 (2), GB2015.
Jarvis, P.G., 1976. The interpretation of the variations in leaf water potential and stomatal conductance found in canopies in the field. Philos. Trans. R. Soc. Lond. Ser. B 273 (927), 593–610.
Keller, M., Varner, R., Dias, J.D., Silva, H., Crill, P., de Oliveira, R.C., Asner, G.P., 2005. Soil–atmosphere exchange of nitrous oxide, nitric oxide, methane, and carbon dioxide in logged and undisturbed forest in the Tapajos National Forest, Brazil. Earth Interact. 9 (23), 1–28.
Krinner, G., Viovy, N., de Noblet-Ducoudré, N., Ogée, J., Polcher, J., Friedlingstein, P., Ciais, P., Sitch, S., Prentice, I.C., 2005. A dynamic global vegetation model for studies of the coupled atmosphere–biosphere system. Global Biogeochem. Cycles 19 (1), GB1015.
Kruijt, B., Elbers, J.A., von Randow, C., Araújo, A.C., Oliveira, P.J., Culf, A., Manzi, A.O., Nobre, A.D., Kabat, P., Moors, E.J., 2004. The robustness of eddy correlation fluxes for Amazon rain forest conditions. Ecol. Appl. 14 (sp4), 101–113.
Kucharik, C.J., Foley, J.A., Delire, C., Fisher, V.A., Coe, M.T., Lenters, J.D., Young-Molling, C., Ramankutty, N., Norman, J.M., Gower, S.T., 2000. Testing the performance of a dynamic global ecosystem model: water balance, carbon balance, and vegetation structure. Global Biogeochem. Cycles 14 (3), 795–825.
Lawrence, D.M., Oleson, K.W., Flanner, M.G., Thornton, P.E., Swenson, S.C., Lawrence, P.J., Zeng, X., Yang, Z.-L., Levis, S., Sakaguchi, K., Bonan, G.B., Slater, A.G., 2011. Parameterization improvements and functional and structural advances in version 4 of the Community Land Model. J. Adv. Model. Earth Syst. 3, 27.
Lawrence, D.M., Slater, A.G., Romanovsky, V.E., Nicolsky, D.J., 2008. Sensitivity of a model projection of near-surface permafrost degradation to soil column depth and representation of soil organic matter. J. Geophys. Res. 113 (F2), F02011.
Lawrence, P.J., Chase, T.N., 2010. Investigating the climate impacts of global land cover change in the Community Climate System Model. Int. J. Clim. 30 (13), 2066–2087.
Lee, J.-E., Oliveira, R.S., Dawson, T.E., Fung, I., 2005. Root functioning modifies seasonal climate. Proc. Natl. Acad. Sci. U.S.A. 102 (49), 17576–17581.
Lee, T.J., 1992. The Impact of Vegetation on the Atmospheric Boundary Layer and Convective Storms. Dept. of Atmospheric Science, Colorado State University, Fort Collins, CO, USA.
Lee, T.J., Pielke, R.A., Kittel, T.G.F., Weaver, J.F., 1993. Atmospheric modeling and its spatial representation of land surface characteristics. In: Goodchild, M., Parks, B., Steyaert, L.T. (Eds.), Environmental Modeling with GIS. Oxford University Press, New York, NY.
Leuning, R., 1995. A critical appraisal of a combined stomatal-photosynthesis model for C_3 plants. Plant Cell Environ. 18 (4), 339–355.
Levis, S., Bonan, G.B., Vertenstein, M., Oleson, K.W., 2004. The Community Land Model's Dynamic Global Vegetation Model (CLM-DGVM): Technical Description and User's Guide. National Center for Atmospheric Research, Boulder, CO, USA.
Levis, S., Coe, M.T., Foley, J.A., 1996. Hydrologic budget of a land surface model: a global application. J. Geophys. Res. 101 (D12), 16921–16930.
Li, W., Fu, R., 2004. Transition of the large-scale atmospheric and land surface conditions from the dry to the wet season over Amazonia as diagnosed by the ECMWF re-analysis. J. Clim. 17 (13), 2637–2651.
Li, W., Fu, R., Dickinson, R.E., 2006. Rainfall and its seasonality over the Amazon in the 21st century as assessed by the coupled models for the IPCC AR4. J. Geophys. Res. 111 (D2), D02111.
Linn, D.M., Doran, J.W., 1984. Effect of water-filled pore space on carbon dioxide and nitrous oxide production in tilled and nontilled soils. Soil Sci. Soc. Am. J. 48 (6), 1267–1272.
Liu, M., Tian, H., Lu, C., Xu, X., Chen, G., Ren, W., 2012. Effects of multiple environment stresses on evapotranspiration and runoff over eastern China. J. Hydrol. 426/427, 39–54.
Lloyd, J., Farquhar, G.D., 1994. ^{13}C discrimination during CO_2 assimilation by the terrestrial biosphere. Oecologia 99 (3), 201–215.
Lloyd, J., Taylor, J.A., 1994. On the temperature dependence of soil respiration. Funct. Ecol. 8 (3), 315–323.
Lu, C., Tian, H., Liu, M., Ren, W., Xu, X., Chen, G., Zhang, C., 2011. Effect of nitrogen deposition on China's terrestrial carbon uptake in the context of multifactor environmental changes. Ecol. Appl. 22 (1), 53–75.
Malhi, Y., Roberts, J.T., Betts, R.A., Killeen, T.J., Li, W., Nobre, C.A., 2008. Climate change, deforestation, and the fate of the Amazon. Science 319 (5860), 169–172.
McWilliam, A.-L.C., Cabral, O.M.R., Gomes, B.M., Esteves, J.L., Roberts, J.M., 1996. Forest and pasture leaf-gas exchange in southwest Amazonia. In: Gash, J.H.C., Nobre, C.A., Roberts, J.M., Victoria, R.L. (Eds.), Amazonian Deforestation and Climate. J. M. Wiley and Sons, New York, NY, USA, pp. 265–286.
Medvigy, D., Wofsy, S.C., Munger, J.W., Hollinger, D.Y., Moorcroft, P.R., 2009. Mechanistic scaling of ecosystem function and dynamics in space and time: ecosystem demography model version 2. J. Geophys. Res. 114 (G1), G01002.
Miguez-Macho, G., Fan, Y., Weaver, C.P., Walko, R., Robock, A., 2007. Incorporating water table dynamics in climate modeling: 2. Formulation, validation, and soil moisture simulation. J. Geophys. Res. 112 (D13), D13108.
Miller, S.D., Goulden, M.L., da Rocha, H.R., 2007. The effect of canopy gaps on subcanopy ventilation and scalar fluxes in a tropical forest. Agric. For. Meteorol. 142 (1), 25–34.
Miller, S.D., Goulden, M.L., Menton, M.C., da Rocha, H.R., de Freitas, H.C., Figueira, A.M.e.S., Dias de Sousa, C.A., 2004. Biometric and micrometeorological measurements of tropical forest carbon balance. Ecol. Appl. 14 (sp4), 114–126.
Monteith, J.L., 1995. Accommodation between transpiring vegetation and the convective boundary layer. J. Hydrol. 166 (3/4), 251–263.
Moorcroft, P.R., Hurtt, G.C., Pacala, S.W., 2001. A method for scaling vegetation dynamics: the ecosystem demography model (ED). Ecol. Monogr. 71 (4), 557–586.
Niu, G.-Y., Yang, Z.-L., Mitchell, K.E., Chen, F., Ek, M.B., Barlage, M., Kumar, A., Manning, K., Niyogi, D., Rosero, E., Tewari, M., Xia, Y., 2011. The community Noah land surface model with multiparameterization options (Noah-MP): 1. Model description and evaluation with local-scale measurements. J. Geophys. Res. 116 (D12), D12109.
Nobre, C.A., Fisch, G., da Rocha, H.R., da, F., Lyra, R.F., da Rocha, E.P., da Costa, A.C.L., Ubarana, V.N., 1996. Observations of the atmospheric boundary layer in Rondônia. In: Gash, J.H.C., Nobre, C.A., Roberts, J.M., Victoria, R.L. (Eds.), Amazonian Deforestation and Climate. J.M. Wiley and Sons, New York, NY, USA, pp. 413–424.
Nobre, C.A., Sellers, P.J., Shukla, J., 1991. Amazonian deforestation and regional climate change. J. Clim. 4 (10), 957–988.
Oleson, K.W., Dai, Y., Bosilovich, M., Dickinson, R., Dirmeyer, P., 2004. Technical Description of the Community Land Model (CLM). National Center for Atmospheric Research, Boulder, CO, USA.
Oleson, K.W., Lawrence, D.M., Bonan, G.B., Flanner, M.G., Kluzek, E., Lawrence, P.J., Levis, S., Swenson, S.C., Thornton, P.E., Decker, M., Dickinson, R., Feddema, J., Heald, C.L., Hoffman, F., Lamarque, J.-F., Mahowald, N., Niu, G.-Y., Qian, T., Randerson, J., Running, S., Sakaguchi, K., Slater, A., Stöckli, R., Wang, A., Liang, Z.-L., Zeng, X., Zeng, X., 2010. Technical Description of Version 4.0 of the Community Land Model (CLM). National Center for Atmospheric Research, Boulder, CO, USA.

Oleson, K.W., Niu, G.Y., Yang, Z.L., Lawrence, D.M., Thornton, P.E., Lawrence, P.J., Stöckli, R., Dickinson, R.E., Bonan, G.B., Levis, S., Dai, A., Qian, T., 2008. Improvements to the Community Land Model and their impact on the hydrological cycle. J. Geophys. Res. 113 (G1), G01021.

Parton, W., Stewart, J., Cole, C., 1988. Dynamics of C, N, P and S in grassland soils: a model. Biogeochemistry 5 (1), 109–131.

Potter, C.S., Randerson, J.T., Field, C.B., Matson, P.A., Vitousek, P.M., Mooney, H.A., Klooster, S.A., 1993. Terrestrial ecosystem production: a process model based on global satellite and surface data. Global Biogeochem. Cycles 7 (4), 811–841.

Priestley, C.H.B., Taylor, R.J., 1972. On the assessment of surface heat flux and evaporation using large scale parameters. Mon. Weather Rev. 100 (2), 81–92.

Randall, D.A., Dazlich, D.A., Zhang, C., Denning, A.S., Sellers, P.J., Tucker, C.J., Bounoua, L., Berry, J.A., Collatz, G.J., Field, C.B., Los, S.O., Justice, C.O., Fung, I., 1996. A revised land surface parameterization (SiB2) for GCMs. Part III: The greening of the Colorado State University general circulation model. J. Clim. 9 (4), 738–763.

Randerson, J.T., Hoffman, F.M., Thornton, P.E., Mahowald, N.M., Lindsay, K., Lee, Y.-H., Nevison, C.D., Doney, S.C., Bonan, G., Stöckli, R., Covey, C., Running, S.W., Fung, I.Y., 2009. Systematic assessment of terrestrial biogeochemistry in coupled climate–carbon models. Global Change Biol. 15 (10), 2462–2484.

Rayner, P.J., Law, R.M., Dargaville, R., 1999. The relationship between tropical CO_2 fluxes and the El Niño Southern Oscillation. Geophys. Res. Lett. 26 (4), 493–496.

Ren, W., Tian, H., Xu, X., Liu, M., Lu, C., Chen, G., Melillo, J., Reilly, J., Liu, J., 2011. Spatial and temporal patterns of CO_2 and CH_4 fluxes in China's croplands in response to multifactor environmental changes. Tellus B 63 (2), 222–240.

Rosolem, R., Shuttleworth, W.J., de Gonçalves, L.G.G., 2008. Is the data collection period of the Large-Scale Biosphere–Atmosphere Experiment in Amazonia representative of long-term climatology? J. Geophys. Res. 113 (G1), G00B09.

Rottenberger, S., Kuhn, U., Wolf, A., Schebeske, G., Oliva, S.T., Tavares, T.M., Kesselmeier, J., 2004. Exchange of short-chain aldehydes between Amazonian vegetation and the atmosphere. Ecol. Appl. 14 (sp4), 247–262.

Ruimy, A., Dedieu, G., Saugier, B., 1996. TURC: a diagnostic model of continental gross primary productivity and net primary productivity. Global Biogeochem. Cycles 10 (2), 269–285.

Ryan, M.G., 1991. A simple method for estimating gross carbon budgets for vegetation in forest ecosystems. Tree Physiol. 9 (1-2), 255–266.

Rödenbeck, C., Houweling, S., Gloor, M., Heimann, M., 2003. CO_2 flux history 1982–2001 inferred from atmospheric data using a global inversion of atmospheric transport. Atmos. Chem. Phys. 3 (6), 1919–1964.

Sakai, R.K., Fitzjarrald, D.R., Moraes, O.L.L., Staebler, R.M., Acevedo, O.C., Czikowsky, M.J., Silva, R.d., Brait, E., Miranda, V., 2004. Land-use change effects on local energy, water, and carbon balances in an Amazonian agricultural field. Global Change Biol. 10 (5), 895–907.

Salazar, L.F., Nobre, C.A., Oyama, M.D., 2007. Climate change consequences on the biome distribution in tropical South America. Geophys. Res. Lett. 34 (9), L09708.

Saleska, S.R., Miller, S.D., Matross, D.M., Goulden, M.L., Wofsy, S.C., da Rocha, H.R., de Camargo, P.B., Crill, P., Daube, B.C., de Freitas, H.C., Hutyra, L., Keller, M., Kirchhoff, V., Menton, M., Munger, J.W., Pyle, E.H., Rice, A.H., Silva, H., 2003. Carbon in Amazon forests: unexpected seasonal fluxes and disturbance-induced losses. Science 302 (5650), 1554–1557.

Santos, S.N.M., Costa, M.H., 2004. A simple tropical ecosystem model of carbon, water and energy fluxes. Ecol. Modell. 176 (3/4), 291–312.

Schaefer, K., Collatz, G.J., Tans, P., Denning, A.S., Baker, I., Berry, J., Prihodko, L., Suits, N., Philpott, A., 2008. Combined simple biosphere/Carnegie-Ames-Stanford approach terrestrial carbon cycle model. J. Geophys. Res. 113 (G3), G03034.

Schaefer, K., Zhang, T., Slater, A.G., Lu, L., Etringer, A., Baker, I., 2009. Improving simulated soil temperatures and soil freeze/thaw at high-latitude regions in the Simple Biosphere/Carnegie-Ames-Stanford Approach model. J. Geophys. Res. 114 (F2), F02021.

Schenk, H.J., Jackson, R.B., 2002. Rooting depths, lateral root spreads and below-ground/above-ground allometries of plants in water-limited ecosystems. J. Ecol. 90 (3), 480–494.

Sellers, P.J., 1985. Canopy reflectance, photosynthesis and transpiration. Int. J. Remote Sens. 6 (8), 1335–1372.

Sellers, P.J., Mintz, Y., Sud, Y.C., Dalcher, A., 1986. A simple biosphere model (SiB) for use within general circulation models. J. Atmos. Sci. 43 (6), 505–531.

Sellers, P.J., Randall, D.A., Collatz, G.J., Berry, J.A., Field, C.B., Dazlich, D.A., Zhang, C., Collelo, G.D., Bounoua, L., 1996. A revised land surface parameterization (SiB2) for atmospheric GCMs. Part I: Model formulation. J. Clim. 9 (4), 676–705.

Shinozaki, K., Yoda, K., Hozumi, K., Kira, T., 1964. A quantitative analysis of plant form. Pipe model theory. I. Basic analysis. Jpn. J. Ecol. 14 (3), 97–105.

Sitch, S., Smith, B., Prentice, I.C., Arneth, A., Bondeau, A., Cramer, W., Kaplan, J.O., Levis, S., Lucht, W., Sykes, M.T., Thonicke, K., Venevsky, S., 2003. Evaluation of ecosystem dynamics, plant geography and terrestrial carbon cycling in the LPJ dynamic global vegetation model. Global Change Biol. 9 (2), 161–185.

Souza Filho, J.D.d.C., Ribeiro, A., Costa, M.H., Cohen, J.C.P., 2005. Control mechanisms of the seasonal variation of transpiration in a northeast Amazonian tropical rainforest (in Portuguese). Acta Amazon. 35 (2), 223–229.

Stephens, B.B., Gurney, K.R., Tans, P.P., Sweeney, C., Peters, W., Bruhwiler, L., Ciais, P., Ramonet, M., Bousquet, P., Nakazawa, T., Aoki, S., Machida, T., Inoue, G., Vinnichenko, N., Lloyd, J., Jordan, A., Heimann, M., Shibistova, O., Langenfelds, R.L., Steele, L.P., Francey, R.J., Denning, A.S., 2007. Weak northern and strong tropical land carbon uptake from vertical profiles of atmospheric CO_2. Science 316 (5832), 1732–1735.

Stöckli, R., Rutishauser, T., Dragoni, D., O'Keefe, J., Thornton, P.E., Jolly, M., Lu, L., Denning, A.S., 2008. Remote sensing data assimilation for a prognostic phenology model. J. Geophys. Res. 113 (G4), G04021.

Tao, Z., Jain, A.K., 2005. Modeling of global biogenic emissions for key indirect greenhouse gases and their response to atmospheric CO_2 increases and changes in land cover and climate. J. Geophys. Res. 110 (D21), D21309.

Thompson, S.L., Pollard, D., 1995a. A global climate model (GENESIS) with a land-surface transfer scheme (LSX). Part I: Present climate simulation. J. Clim. 8 (4), 732–761.

Thompson, S.L., Pollard, D., 1995b. A global climate model (GENESIS) with a land-surface transfer scheme (LSX). Part II: CO_2 sensitivity. J. Clim. 8 (5), 1104–1121.

Thornton, P.E., Doney, S.C., Lindsay, K., Moore, J.K., Mahowald, N., Randerson, J.T., Fung, I., Lamarque, J.F., Feddema, J.J., Lee, Y.H., 2009. Carbon–nitrogen interactions regulate climate–carbon cycle feedbacks: results from an atmosphere–ocean general circulation model. Biogeosciences 6 (10), 2099–2120.

Thornton, P.E., Lamarque, J.-F., Rosenbloom, N.A., Mahowald, N.M., 2007. Influence of carbon–nitrogen cycle coupling on land model response to CO_2 fertilization and climate variability. Global Biogeochem. Cycles 21 (4), GB4018.

Thornton, P.E., Law, B.E., Gholz, H.L., Clark, K.L., Falge, E., Ellsworth, D.S., Goldstein, A.H., Monson, R.K., Hollinger, D., Falk, M., Chen, J., Sparks, J.P., 2002. Modeling and measuring the effects of disturbance history and climate on carbon and water budgets in evergreen needleleaf forests. Agric. For Meteorol. 113 (1–4), 185–222.

Thornton, P.E., Rosenbloom, N.A., 2005. Ecosystem model spin-up: estimating steady state conditions in a coupled terrestrial carbon and nitrogen cycle model. Ecol. Modell. 189 (1/2), 25–48.

Tian, H., Chen, G., Liu, M., Zhang, C., Sun, G., Lu, C., Xu, X., Ren, W., Pan, S., Chappelka, A., 2010a. Model estimates of net primary productivity, evapotranspiration, and water use efficiency in the terrestrial ecosystems of the southern United States during 1895–2007. Forest Ecol. Manage. 259 (7), 1311–1327.

Tian, H., Chen, G., Zhang, C., Liu, M., Sun, G., Chappelka, A., Ren, W., Xu, X., Lu, C., Pan, S., Chen, H., Hui, D., McNulty, S., Lockaby, G., Vance, E., 2012. Century-scale responses of ecosystem carbon storage and flux to multiple environmental changes in the Southern United States. Ecosystems 15 (4), 674–694.

Tian, H., Melillo, J., Lu, C., Kicklighter, D., Liu, M., Ren, W., Xu, X., Chen, G., Zhang, C., Pan, S., Liu, J., Running, S., 2011a. China's terrestrial carbon balance: contributions from multiple global change factors. Global Biogeochem. Cycles 25 (1), GB1007.

Tian, H., Melillo, J.M., Kicklighter, D.W., McGuire, A.D., Helfrich III, J., Moore III, B., Vörösmarty, C.J., 2000. Climatic and biotic controls on annual carbon storage in Amazonian ecosystems. Global Ecol. Biogeogr. 9 (4), 315–335.

Tian, H., Xu, X., Liu, M., Ren, W., Zhang, C., Chen, G., Lu, C., 2010b. Spatial and temporal patterns of CH_4 and N_2O fluxes in terrestrial ecosystems of North America during 1979–2008: application of a global biogeochemistry model. Biogeosciences 7 (9), 2673–2694.

Tian, H., Xu, X., Liu, M., Ren, W., Zhang, C., Chen, G., Lu, C., 2011b. Net exchanges of CO_2, CH_4, and N_2O between China's terrestrial ecosystems and the atmosphere and their contributions to global climate warming. J. Geophys. Res. 116 (G2), G02011.

van den Hurk, B.J.J.M., Viterbo, P., Beljaars, A.C.M., Betts, A.K., 2000. Offline Validation of the ERA40 Surface Scheme. European Centre for Medium-Range Weather Forecasts, Reading, UK.

Verbeeck, H., Peylin, P., Bacour, C., Bonal, D., Steppe, K., Ciais, P., 2011. Seasonal patterns of CO_2 fluxes in Amazon forests: fusion of eddy covariance data and the ORCHIDEE model. J. Geophys. Res. 116 (G2), G02018.

Verseghy, D.L., 2000. The Canadian land surface scheme (CLASS): its history and future. Atmos. Ocean 38 (1), 1–13.

Verseghy, D.L., McFarlane, N.A., Lazare, M., 1993. Class—a Canadian land surface scheme for GCMS, II. Vegetation model and coupled runs. Int. J. Clim. 13 (4), 347–370.

Vidale, P.L., Stöckli, R., 2005. Prognostic canopy air space solutions for land surface exchanges. Theor. Appl. Climatol. 80 (2), 245–257.

von Randow, C., Manzi, A.O., Kruijt, B., de Oliveira, P.J., Zanchi, F.B., Silva, R.L., Hodnett, M.G., Gash, J.H.C., Elbers, J.A., Waterloo, M.J., Cardoso, F.L., Kabat, P., 2004. Comparative measurements and seasonal variations in energy and carbon exchange over forest and pasture in South West Amazonia. Theor. Appl. Climatol. 78 (1), 5–26.

Walko, R.L., Band, L.E., Baron, J., Kittel, T.G.F., Lammers, R., Lee, T.J., Ojima, D., Pielke, R.A., Taylor, C., Tague, C., Tremback, C.J., Vidale, P.L., 2000. Coupled atmosphere–biophysics–hydrology models for environmental modeling. J. Appl. Meteorol. 39 (6), 931–944.

Werth, D., Avissar, R., 2002. The local and global effects of Amazon deforestation. J. Geophys. Res. 107 (D20), 8087.

White, M.A., Thornton, P.E., Running, S.W., 1997. A continental phenology model for monitoring vegetation responses to interannual climatic variability. Global Biogeochem. Cycles 11 (2), 217–234.

White, M.A., Thornton, P.E., Running, S.W., Nemani, R.R., 2000. Parameterization and sensitivity analysis of the BIOME–BGC terrestrial ecosystem model: net primary production controls. Earth Interact. 4 (3), 1–85.

Wigmosta, M.S., Vail, L.W., Lettenmaier, D.P., 1994. A distributed hydrology–vegetation model for complex terrain. Water Resour. Res. 30 (6), 1665–1679.

Williams, M., Shimabukuro, Y.E., Herbert, D.A., Pardi Lacruz, S., Renno, C., Rastetter, E.B., 2002. Heterogeneity of soils and vegetation in an Eastern Amazonian rain forest: implications for scaling up biomass and production. Ecosystems 5 (7), 0692–0704.

Xue, Y., Sellers, P.J., Kinter, J.L., Shukla, J., 1991. A simplified biosphere model for global climate studies. J. Clim. 4 (3), 345–364.

Yang, X., Wittig, V., Jain, A.K., Post, W., 2009. Integration of nitrogen cycle dynamics into the Integrated Science Assessment Model for the study of terrestrial ecosystem responses to global change. Global Biogeochem. Cycles 23 (4), GB4029.

Yang, Z.-L., Cai, X., Zhang, G., Tavakoly, A.A., Jin, O., Meyer, L.H., Guan, X., 2011. The Community Noah Land Surface Model with Multi-Parameterization Options (Noah-MP): Technical Description. Center for Earth System Sciences, The University of Texas at Austin, Austin, TX.

Yang, Z.-L., Niu, G.-Y., 2003. The Versatile Integrator of Surface and Atmosphere processes: Part 1. Model description. Global Planet. Change 38 (1/2), 175–189.

Yuan, F., Arain, M.A., Barr, A.G., Black, T.A., Bourque, C.P.A., Coursolle, C., Margolis, H.A., McCaughey, J.H., Wofsy, S.C., 2008. Modeling analysis of primary controls on net ecosystem productivity of seven boreal and temperate coniferous forests across a continental transect. Global Change Biol. 14 (8), 1765–1784.

Zeng, X., 2001. Global vegetation root distribution for land modeling. J. Hydrometeorol. 2 (5), 525–530.

Zeng, X., Zhao, M., Dickinson, R.E., 1998. Intercomparison of bulk aerodynamic algorithms for the computation of sea surface fluxes using TOGA COARE and TAO data. J. Clim. 11 (10), 2628–2644.

Zhan, X., Xue, Y., Collatz, G.J., 2003. An analytical approach for estimating CO_2 and heat fluxes over the Amazonian region. Ecol. Modell. 162 (1/2), 97–117.